Dalton Transactions

ROYAL SOCIETY OF CHEMISTRY

PERSPECTIVE

View Article Online
View Journal | View Issue

Cite this: *Dalton Trans.*, 2025, **54**, 12714

Engineering of abundant metal complexes for electrochemical water splitting

Naseem Kousar, Gouthami Patil, Ashwini Chikkabasur Kumbara, Basavesh Nisty, Rajesh G. H. and Lokesh Koodlur Sannegowda *

Advancements in water splitting technologies are crucial for achieving sustainable hydrogen production. Development of highly efficient and economically viable catalysts is essential for commercialization of water electrolysers. While precious metals like platinum and iridium are renowned for their catalytic capabilities in the hydrogen evolution reaction (HER) and oxygen evolution reaction (OER), their high cost and scarcity present significant challenges. Hence, various metal oxides, carbides, sulfides, phosphides, alloys, metal complexes, and composites have been examined as potential catalysts for water splitting reactions. This review offers a comprehensive analysis of Earth-abundant metal complexes as promising alternatives for water splitting catalysis. The fundamental principles underlying water splitting, including electrochemical dynamics, thermodynamics, and reaction kinetics, and their impact on catalytic performance have been evaluated. Emphasis is placed on the pivotal role of Earth-abundant metals such as manganese, iron, cobalt, nickel, and molybdenum and their recent innovations in catalyst design focussing on composites for enhancing the HER, OER, and integrated dual-function catalysis are discussed. Comparative evaluation related to advantages and limitations of these alternatives with respect to precious catalysts in terms of cost, availability, and environmental impact is presented. To integrate the same catalyst for HER and OER activities, insights into strategies for optimization of the performance are provided. Additionally, the review highlights the contributions of computational chemistry, including density functional theory studies in engineering catalyst design and understanding reaction mechanisms. Finally, an assessment of current challenges and future directions is presented to provide a holistic perspective on the transformative potential of Earth-abundant metal complexes in advancing sustainable water splitting technologies.

Received 18th June 2025,
Accepted 22nd July 2025

DOI: 10.1039/d5dt01438g

rsc.li/dalton

1. Introduction

The advancement of sustainable, scalable, and efficient technologies for the production of clean fuels is essential to achieve a global shift towards a decarbonized economy and to attain an important milestone in reducing climate change.[1] Hydrogen has enormous potential as a green fuel with high energy density and a distinct advantage of producing only water as a byproduct during combustion.[2,3] Hydrogen produced from renewable resources acts as a sustainable substitute for fossil fuels and promotes decarbonization of effluents in various domains like chemical manufacturing, steel production, and robust transportation.[4–6] Despite its potential, most of the hydrogen produced worldwide today (>95%) comes from thermochemical processes like coal gasification and steam methane reforming. However, these traditional routes erode the very purpose of sustainability since they are expensive, energy-intensive, and carbon-emitting.[2,7]

In contrast to this, electrochemical water splitting (EWS), in which water splits into molecular hydrogen (H_2) and oxygen (O_2) utilizing electricity derived from renewable energy sources, has emerged as a monumental approach for generating hydrogen.[8] Being naturally carbon-neutral, this green hydrogen pathway presents an opportunity for decentralized hydrogen production by coupling with the periodic renewable energy sources. The hydrogen evolution reaction (HER) at the cathode and the oxygen evolution reaction (OER) at the anode are the two half-reactions responsible for EWS.[9,10] Both the reactions, though appearing straightforward, are thermodynamically and kinetically challenging resulting in the requirement of significant activation energies.[11] To overcome the slow reaction kinetics along with substantial energy losses, efficient catalysts are used for both the

Department of Studies in Chemistry, Vijayanagara Sri Krishnadevaraya University, Jnanasagara Campus, Vinayakanagara, Ballari-583105, Karnataka, India. E-mail: kslokesh@vskub.ac.in, naseem.kousar9999@gmail.com, gouthamipatil6@gmail.com, ashwindilip88@gmail.com, basavesh.nisty@gmail.com, rajeshgh95.rgh@gmail.com; Tel: +91 9035500208

HER and OER and the efficiency of the catalysts has a significant impact on the performance of water electrolyzers.[3,7] Although noble metals like platinum (Pt) for the HER and ruthenium (Ru) or iridium (Ir) oxides for the OER have been the standard catalysts for years due to their impressive catalytic activity, they have an array of drawbacks. Since these metals are expensive, rare, uni-functional, and their activity swiftly diminishes by electrochemical processes, their viability and versatility are confined. Furthermore, their comparatively inflexible electronic structure restricts the possibilities of optimization through structural or molecular engineering and in turn limits the ability to tune their catalytic properties.[11,12]

Beyond molecular engineering, the designed catalysts need to be scalable and cost-effective for practical application of EWS technologies. A recent techno-economic analysis revealed that stack components and catalysts contribute to more than 50% of the overall electrolyzer cost, emphasizing the urgent need for Earth-abundant and high-performance bifunctional materials.[13] Additionally, the demand for distinct individual catalysts for the HER and OER causes system construction even more complicated and raises expenses. Bifunctional electrocatalysts can effectively catalyze both HER and OER, and hence a lot of curiosity is drawn as a potential remedy to these challenges.[14] These materials advance performance, simplify device construction, and lessen component count for water electrolyzers and unitize renewable fuel cells.[15] The design of bifunctional catalysts is inherently difficult because the OER and HER necessitate distinctive active site features and operate *via* different mechanisms.[11] The OER involves a complex four-electron oxidation process with higher thermodynamic and kinetic barriers, whereas the HER usually involves rapid proton-coupled electron transfer (PCET) steps in either acidic or alka-

Naseem Kousar

Naseem Kousar obtained her M. Sc. in Chemistry from the University of Mysore and recently completed her Ph.D. at Vijayanagara Sri Krishnadevaraya University, Ballari, under the supervision of Prof. K. S. Lokesh. Her doctoral research centered on the rational design of macrocyclic redox-active complexes, with a focus on tailoring their electronic structure and interfacial characteristics for applications in water electrolysis and bifunctional oxygen electrocatalysis (OER/ORR). She has worked extensively on metal phthalocyanine-based hybrids, integrating them with conductive nanocarbon scaffolds to engineer efficient and durable electrocatalysts through synergistic interface modulation. Her work has contributed to a mechanistic understanding of structure–activity relationships in hybrid electrocatalytic systems, combining synthetic development with electrochemical and spectroscopic characterization. She has disseminated her findings through multiple research articles published in reputed international journals, reflecting her sustained contributions to the field of molecular electrocatalysis and hybrid materials. In recognition of her research excellence, she has received several distinctions, including the DST Ph.D. Fellowship (Government of Karnataka), the Young Scientist Award from the Indian Academy of Physical Sciences, the Research Award of Excellence from VOICE India, and the Elsevier Best Paper Award conferred by the Inter-University Centre for Nanomaterials and Devices (CUSAT, India). She was also selected by the Department of Science and Technology, Government of India, to represent the country at the 74th Lindau Nobel Laureate Meeting (Chemistry) in 2025. Her research interests lie at the intersection of molecular electrocatalysis, interfacial charge transfer, and hybrid material engineering for next-generation sustainable energy technologies.

Gouthami Patil

Gouthami Patil completed her M.Sc. in Chemistry with first rank from Vijayanagara Sri Krishnadevaraya University, Ballari, where she is currently pursuing her Ph.D. under the supervision of Prof. K. S. Lokesh. Her doctoral research focuses on the design and development of bio-inspired redox-active molecules, with an emphasis on their electrochemical properties and catalytic applications in sustainable energy conversion. Her work integrates molecular design with functional electrochemistry to develop advanced electrocatalytic systems. She has shared her findings through publications in international journals and active participation in national and global scientific forums. In recognition of her academic merit and research promise, she was awarded the DST INSPIRE Fellowship by the Department of Science and Technology, Government of India. She was also selected to represent India at the 74th Lindau Nobel Laureate Meeting (Chemistry), 2025, highlighting her growing visibility in the international research community. Her research interests include redox catalysis, electrochemical energy systems, and the development of molecular materials for clean energy technologies.

line media.[16,17] Therefore, catalysts with adjustable electronic structures, multiple accessible oxidative states, substantial surface area, and robustness in structure under varying redox scenarios are needed to achieve optimal bifunctionality.[14]

Over the last decade, researchers have focused on electrocatalysts composed of Earth-abundant transition metals such as manganese (Mn), iron (Fe), cobalt (Co), nickel (Ni), and molybdenum (Mo), which have made substantial advances as noble metal substitutes. These transition-metal-based catalysts provide high catalytic efficiency while remaining cost-effective, abundant, and sustainable.[18,19] Particularly, the rich redox-chemistry of these transition metals, along with their variety of oxidation states, allow them to take part in multi-electron transfer and PCET processes, which are necessary for EWS reactions. Because of these intrinsic characteristics of transition metals, molecular design techniques such as ligand alterations, doping with heteroatoms, optimization in the coordination environment, and integration with conductive supports can be used to specifically change their electronic and structural properties for tuning the catalytic properties.[20,21] For example, Mn is used for the OER, particularly in alkaline media by utilizing its wide range of oxidation states (Mn^{2+} to Mn^{7+}) through nano-structuring and doping.[22] When iron is embedded in N-doped supports or macrocyclic ligands, the redox pair of Fe^{2+}/Fe^{3+} exhibits increased activity.[23] Through hybridization and ligand modulation, Co performance is adjusted to access Co^{2+}/Co^{3+} states.[24] Through alloying (such as NiFe) and support coupling, Ni^{2+}–Ni^{4+} transitions of Ni are empowered which strengthens the activity for the OER in alkaline medium.[25] Mo forms effective bifunctional hybrids like NiMo and CoMo and excels in the HER through active edge sites in MoS_2.[26,27]

Among the various material platforms based on transition metals, metal complexes are unique due to their structural flexibility and molecular reliability. These complexes provide atomically defined coordination spheres around the metal center, offering precise control over the oxidation state, electron density, and geometry, in contrast to bulk metal oxides or alloys.[28] This ability to fine-tune the metal center is essential for adjusting the important catalytic descriptors that regulate the effectiveness and selectivity of EWS reactions, such as intermediate adsorption energies, redox potentials, and PCET kinetics.[21,29] The molecular makeup of the complex also helps in conducting through structure–activity correlation studies, which yield mechanistic insights that are challenging to discover in heterogeneous systems. The logical design of next-generation catalysts with desired performance characteristics will be greatly benefitted from such insights.[30,31] Redox flexibility is another characteristic that makes metal complexes highly desirable. It enables them to participate in multi-electron transformations and stabilize high-energy intermediates during catalytic turnover.[32] By integrating them into hybrid systems with conductive frameworks like graphene, carbon nanotubes, or porous matrix structures, their activity can be further increased.[11] These hybrids elevate electrochemical active surface area, boost charge transport, and induce synergistic interactions, which ultimately result in increased durability and bifunctionality.[3,11] They are especially attractive for practical applications in unitized electrolyzer–fuel cell systems and renewable energy devices due to their configurable and designable architecture.[15,33] In view of these beneficial features, Earth-abundant metal complexes have evolved as an exciting category of bifunctional electrocatalysts that can effectively drive both the OER and HER in EWS. This review discusses recent advances in the design of such complexes and hybrid derivatives (Fig. 1).

Ashwini Chikkabasur Kumbara

Ashwini Chikkabasur Kumbara completed her M.Sc. in Chemistry from Vijayanagara Sri Krishnadevaraya University, Ballari. She is currently pursuing her Ph.D. at the same institution under the supervision of Prof. K. S. Lokesh. Her doctoral research focuses on the development of novel N_4-macrocyclic systems as efficient catalysts for electrochemical applications, with an emphasis on structural innovation and performance optimization. Her work aims to advance the field by exploring new molecular architectures and mechanistic pathways for improved electrocatalytic performance. She has communicated her research findings through publications in reputed international journals, reflecting her active engagement with the scientific community and commitment to the progression of electrochemical sciences.

Basavesh Nisty

Basavesh Nisty completed both his B.Sc. and M.Sc. degrees in Chemistry from Vijayanagara Sri Krishnadevaraya University, Ballari. He is currently pursuing his Ph.D. at the same institution under the supervision of Prof. K. S. Lokesh. His doctoral research is focused on clean and sustainable energy technologies, with particular emphasis on the electrochemical production of hydrogen through water splitting. His work aims to contribute to the development of efficient and cost-effective electrocatalytic systems for green hydrogen generation. His research reflects growing interest in addressing global energy challenges through innovative electrochemical strategies.

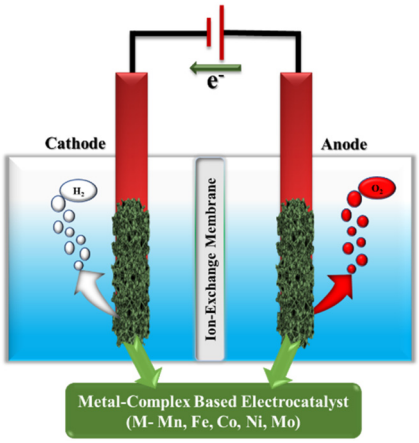

Fig. 1 Graphical representation of EWS with Earth-abundant metal complex-based electrocatalysts.

Special attention is paid to the design principles, structure–function relationships, and mechanistic understanding that support their catalytic function. Furthermore, the multi-metallic systems and synergistic approaches that improve stability and activity in a range of operational conditions have been discussed. The ultimate goal of this review is to provide a comprehensive overview and identify future research directions concerning the role of metal complexes in the evolving field of sustainable hydrogen production technologies.

2. Mechanistic fundamentals of electrochemical water splitting

Sustainable hydrogen production using EWS requires overcoming of the kinetic and thermodynamic barriers tied with the HER and OER. An efficient molecular design framework for tackling these problems is offered by transition metal com-

Rajesh G. H.

Rajesh G. H. completed his Bachelor's degree from Laxmi Venkatesh Desai College, Raichur, and earned his M.Sc. in Chemistry from Gulbarga University, Kalaburagi. He is currently pursuing his Ph.D. at Vijayanagara Sri Krishnadevaraya University, Ballari, under the supervision of Prof. K. S. Lokesh. His research focuses on interfacial electrochemistry with an emphasis on energy conversion and storage devices. His work aims to advance the understanding of electrode–electrolyte interactions and develop efficient materials for next-generation sustainable energy systems.

Lokesh Koodlur Sannegowda

Lokesh Koodlur Sannegowda is a Professor of Chemistry at Vijayanagara Sri Krishnadevaraya University, Ballari, India. He obtained his M.Sc. in Chemistry from the University of Mysore, and earned his Ph.D. from the same institution under the guidance of Prof. B. N. Achar, working on metal phthalocyanines and their polymers as molecular conductors. He has held postdoctoral positions and visiting scientist roles in France, Belgium, and Japan, and currently leads an active research group focused on redox-active macrocycles, electrocatalysis, and electrochemical energy conversion. His research integrates molecular design, interfacial electrochemistry, and hybrid materials for sustainable technologies, particularly targeting hydrogen evolution, oxygen evolution, and oxygen reduction reactions. He has authored more than 120 publications in internationally reputed journals and holds patents on catalytic materials. He has successfully guided 12 Ph.D. students and currently supervises several doctoral researchers. His group's work has been supported by various national and international agencies, including DST-SERB, VGST, UGC-DAE, and DST-FIST. Dr Lokesh is a Fellow of the Royal Society of Chemistry (FRSC), and has received numerous recognitions including the Sir C.V. Raman Young Scientist Award, CRS Bronze Medal, and several Best Paper Awards. He was a TWAS-UNESCO Associate, and regularly serves as an invited speaker and expert reviewer for high-impact journals such as Angewandte Chemie, Journal of Materials Chemistry A, and Electrochimica Acta. His research continues to contribute significantly to the advancement of electrochemical energy systems and sustainable catalysis.

plexes, in which the metal ions are widely available on Earth and have flexible coordination environments, tailored electronic structures, and enhanced proton–electron transfer pathways. In this section, the HER and OER are thoroughly analyzed mechanistically within the framework of established density functional theory (DFT) methodologies with particular attention to PCET, metal–ligand orbital control, kinetic scaling, electrolyte influence, and energy landscape considerations (Fig. 2).

2.1. The kinetic and thermodynamic aspects

The mechanistic delicacy and electronic fine-tuning of Earth-abundant metal complexes are crucial for EWS. A smooth integration of kinetic modelling, electronic structure regulation, interface design, and thermodynamic insights is essential to achieve optimum catalytic efficiency. Under standard conditions (298 K, 1 atm, pH 0), water splitting require a Gibbs free energy input of 237.2 kJ mol^{-1} at its basic limit, which results in an essential cell voltage of 1.23 V.[7,34] This value corresponds to the difference between the oxygen evolution potential (+1.23 V *versus* the reversible hydrogen electrode, RHE) and the standard hydrogen electrode (SHE, 0.00 V). The Nernst equation (eqn (1)) governs the half-reaction potential's pH dependence:

$$E = E^\circ - \frac{2.303RT}{nF} \times \mathrm{pH} \quad (1)$$

where E is the electrode potential (V), E° is the standard electrode potential, R is the universal gas constant (8.314 J mol^{-1} K^{-1}), T is the temperature (K), n is the number of electrons transferred, and F is Faraday's constant (96 485 C mol^{-1}). At 298 K and n = 1, eqn (1) simplifies to eqn (2), which demonstrates that while the total cell voltage requirement remains unchanged across pH, each half-reaction shifts by about 59 mV per pH unit.[35]

$$E = E^\circ - 0.059 \times \mathrm{pH} \quad (2)$$

Despite this advantageous thermodynamic start point, kinetic barriers and mass transport constraints usually cause practical electrolyzers to function at 1.6–2.0 V. This extra voltage, known as the overpotential (η, eqn (3)), is the energy required to overcome the catalytic cycle's largest free energy barrier (ΔG_{max}).[36]

$$\eta = \frac{\Delta G_{max}}{nF} - E^\circ \quad (3)$$

In order to design effective catalysts, it is essential to minimize ΔG_{max}. This has been investigated systematically using volcano plots and free energy diagrams based on the binding strengths of intermediates like H, OH, and OOH*. Redox-flexible ligands containing transition metals exhibit improved kinetics by reducing the activation barriers of reactions. Moreover, cooperative interactions in multinuclear metal complexes have demonstrated potential for distributing oxidative load, stabilizing transition states, and adjusting electron density, all of which enhance the activity and long-term resilience in challenging electrochemical environments.[37] As a

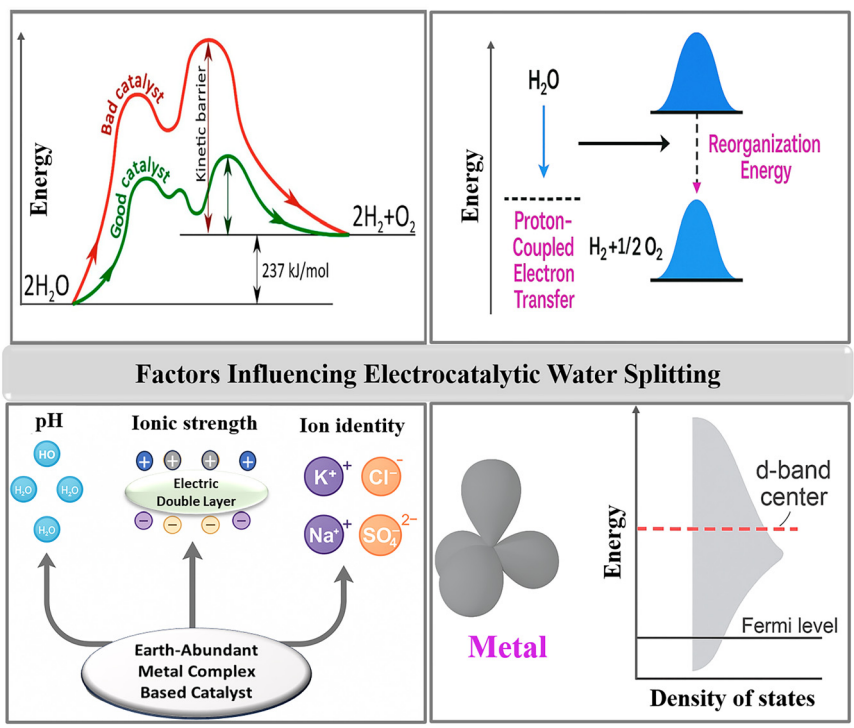

Fig. 2 Overview of key factors influencing EWS.

result, effective catalyst design requires identifying these kinetic bottlenecks and creating materials that reduce them.

2.2. Elementary reaction pathways in acidic and alkaline media

Different mechanistic pathways govern the HER depending on whether the system is operating in an alkaline or acidic environment (Fig. 3). When protons are readily available in acidic media, the HER mechanism typically starts with a proton electrochemically adhering to the catalytic surface to form a metal-bound hydrogen intermediate (H*). This process is referred to as the Volmer step. Then, the reaction proceeds in one of the two ways: either by a chemical recombination route called the Tafel step, in which two nearest H* species combine to form H_2 and rejuvenate the empty catalytic sites, or by an electrochemical desorption process called the Heyrovsky step, in which the adsorbed hydrogen fuses with another proton and electron to release H_2. While the general process is the same in alkaline systems, the proton source is water molecule rather than free hydronium ion.[38] In alkaline media, the Volmer step occurs when the catalytic site helps in water dissociation to H* and hydroxide (OH^-), which eventually discharges H_2 *via* the Heyrovsky or Tafel pathways. It is crucial to design catalysts that can effectively mediate proton generation from water because the additional energetic cost of water dissociation in alkaline media imposes a significant kinetic barrier.[39] These distinctions between the HER mechanisms of acids and bases clarify why catalysts frequently exhibit different efficiencies and activities across pH ranges.

On the other hand, the OER, which involves a four-electron, four-proton transformation, is intrinsically more complicated (Fig. 4). Water adsorption at the catalytic site initiates the OER in acidic environments. Subsequent deprotonation and oxidation processes result in the production of metal–hydroxyl (OH*), metal–oxo (O*), and metal–hydroperoxo (OOH*) intermediates prior to O_2 release. OH^- ions adsorb onto the catalyst surface under alkaline conditions, where they undergo oxidation to form similar OH*, O*, and OOH* intermediates prior to oxygen evolution.[40] Recent mechanistic studies using isotope labelling and operando spectroscopy have revealed distinct energetic pathways for the OER in alkaline systems, where the deprotonation of OH^- and formation of M–OOH intermediates govern the rate.[41] Although acidic and alkaline systems share a general mechanistic framework, the nature of crucial intermediary molecules, proton–electron coupling, and interfacial dynamics are affected by the different proton and oxygen sources, requiring tailored catalyst designs that carefully consider these differences.

2.3. Proton-coupled electron transfer and reorganization energy

The PCET is a crucial component of both the HER and OER, in which electrons and protons navigate together or separately at each step during the reaction. The performance of this step is crucial because the slow reaction and poor catalyst performance result from inefficient proton and electron transfer.[42] The PCET rate (eqn (4)) is influenced by a number of factors, including the reorganization energy, which is necessary for the catalyst and the surrounding solvent to adapt during the reaction. This reorganization energy can be reduced by integrating ligands that support appropriate electronic states or maintain the catalyst's structure, which accelerates the reaction.[43,44] Strategies such as intramolecular hydrogen bonding, redox-active ligands, and rigid chelating scaffolds have been employed to reduce reorganization energy and facilitate synchronous PCET steps in metal complexes.[45]

$$\kappa_{\mathrm{PCET}}\alpha \exp\left(-\frac{(\Delta G^{\circ}+\lambda)^2}{4\lambda\kappa_{\mathrm{B}}T}\right) \quad (4)$$

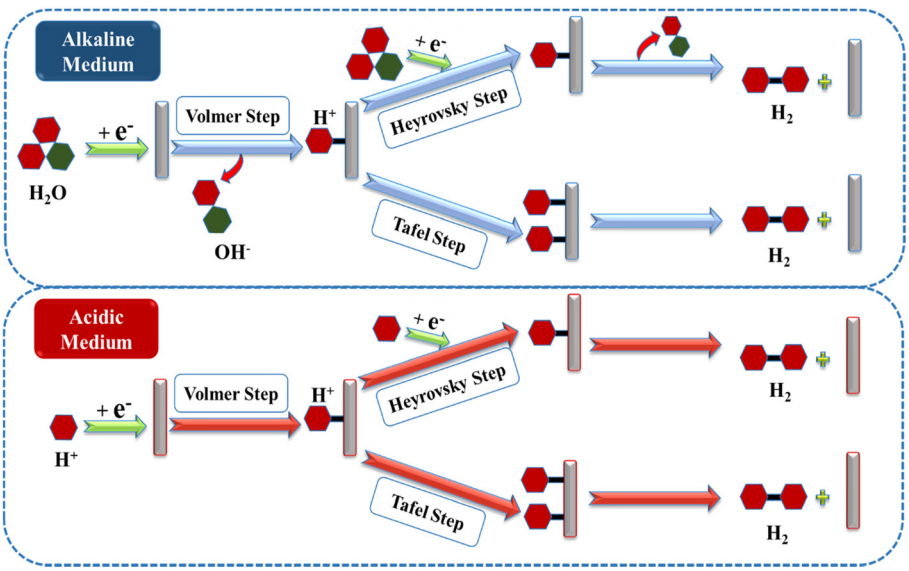

Fig. 3 Mechanistic pathway of the HER in alkaline and acidic media.

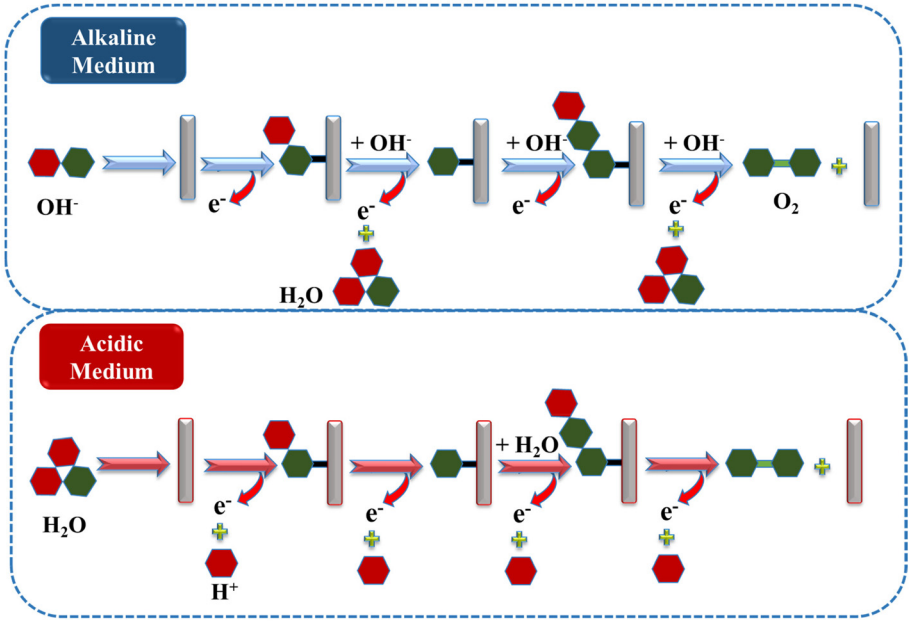

Fig. 4 Mechanistic pathway of the OER in alkaline and acidic media.

where ΔG° is the Gibbs free energy change, λ is the reorganization energy, k_B is Boltzmann's constant, and T is temperature.

2.4. Electronic structure effects and d-band center modulation

An additional crucial design parameter is the d-band center, which is the normalized mean energy of the metal d-states in relation to the Fermi level. Despite being originally established for metallic surfaces, this notion is becoming even more applicable to anchored and molecular catalysts. Adsorbate binding is typically stronger when the d-band center is at a higher level (nearer to the Fermi level), whereas the interaction strength is weakened when the d-band center is at lower level.[46] By adjusting the d-band center, the balance in adsorption and desorption can be achieved during the HER by ensuring that the hydrogen adsorption free energy (ΔG_H) approaches the ideal ~0 eV. In the case of the OER, altering the d-band significantly impacts the overpotentials and reaction rates by modulating the binding strengths of reaction intermediates.[47,48] A strong tuning knob is offered by ligand selection *i.e.*, π-acceptor ligands lower the d-band by stabilizing the d-orbitals through back-donation, while strong σ-donor ligands raise it by donating electron density to the metal center.[49] In addition, anchoring macrocyclic complexes onto conductive supports has been shown to adjust the metal's d-band *via* interfacial electronic coupling, thereby optimizing intermediate binding energy and turnover frequencies.[50] Importantly, during catalysis, many OER catalysts encounter spin-state transitions, such as high-spin M–OH to low-spin M═O species, which may impede turnover and introduce reorganization consequences. In order to reduce these roadblocks and increase efficiency, ligand scaffolds that maintain constant spin states throughout the redox transitions are employed.[51]

2.5. Electrolyte interactions and interfacial phenomena

The regulation of mass transport, ionic strength, ion identity, pH, and electrolyte composition significantly influences the catalytic behaviour. Alkaline electrolytes impede the additional difficulty of water dissociation, requiring catalysts that can efficiently handle OH^-, while acidic electrolytes supply an abundance of protons, promoting the HER.[52] By avoiding pH gradients that could impede turnover or accelerate degradation, buffered electrolytes maintain a specific pH near the electrode. Reactive intermediate stabilization, potential falls, and localized electrostatic environments are all impacted by specific cation and anion effects (*i.e.*, K^+, Na^+, Cl^-, and SO_4^{2-}) that modulate the electrical double layer.[53,54] Additionally mass transport restrictions, gas bubble formation, and concentration variations introduce additional kinetic and transport constraints at high current densities. It has been noticed that the customized interface design utilizing hydrophilic ligand motifs and mesoporous architectures enhances the durability by improving gas bubble release and electrolyte accessibility during EWS.[13] Under dynamic operating conditions, these interfacial techniques aid in preserving stable reaction environments and reduce degradation possibility. Ultimately, charged species such as M–OH or M═O can be stabilized by solvation and hydrogen bonding effects.[55]

2.6. Kinetic-energy constraints shaping activity–stability profiles

The kinetics augmenting interactions are interconnected with the intermediate binding energies and cannot be separately

tuned, which inevitably limit the performance of the catalyst.[56] The Sabatier principle states that highly efficient catalysts adjust intermediate binding strengths to maximize turnover which is governed by volcano-shaped activity plots, for instance, by strong M–OH binding frequency correlating with strong M–OOH binding.[57] However, since strongly binding catalysts may experience oxidative damage, ligand separation, or leaching of metals under operating conditions, optimizing intrinsic activity must be meticulously balanced with maintaining long-term stability.[58] Table 1 provides a comprehensive overview of the essential thermodynamic, kinetic, and electronic characteristics that characterize the HER, OER, and overall EWS.

2.7. Density functional theory and the design principles for molecular catalysts

As an important tool for obtaining mechanistic information, DFT provides an in-depth atomistic understanding of the electronic structure, reaction barriers, and catalytic kinetics. Free energy visualizations derived from DFT calculations offer measurable targets by identifying theoretical overpotentials and potential-determining steps. The primary descriptor of the HER is ΔG_H, ideally close to 0 eV. For the OER, the important PCET steps like ΔG_{OH}, ΔG_O, and ΔG_{OOH} should all approach ~1.23 eV to distribute the energy load equally.[59,60] In addition, DFT also guides the selection of ligands and metals by providing information on spin-state distributions, activation energy environments, frontier orbital energy sources, and d-band roles. DFT insights allow for organized catalyst screening and effective optimization when combined with experimental standards like the overpotential, Tafel slope, TOF, FE, and TON.[51] Recent advances in multiscale modelling have enabled simulation of explicit solvent effects and interfacial charge polarization, refining the accuracy of predicted energy barriers and PCET kinetics in molecular electrocatalysts.[45]

2.8. Characteristic features of catalysts enabling bifunctional water splitting

In order to balance the different mechanistic requirements of the HER and OER, catalysts that facilitate bifunctional water splitting must have a common set of characteristics. The HER usually demands low-valent, electron-rich metal centers that allow for easy proton reduction through transient M–H species with near-thermoneutral adsorption free energy ($\Delta G_{H^*} \approx 0$ eV).[61] On the other hand, the OER implies recurrent proton-coupled electron transfers *via* high-valent intermediates (*OH, *O, and *OOH), required for oxidative stability, multielectron redox resources, and adequate metal–ligand orbital overlap to foster the formation of O–O bonds.[57] Both reductive and oxidative electrochemical inequalities require bifunctional catalysts to have a robust coordination geometry, reduced inner-sphere reorganization, and broad redox tunability in order to facilitate both reactions.[21]

To address this duality, bifunctionality in molecular systems is frequently achieved by means of precisely designed ligand fields that stabilize both the HER and OER-relevant intermediates, while modulating electronic density at the metal site.[33,62] Further improving PCET efficiency, lowering activation barriers, and stabilizing high-energy transition states can be accomplished by redox-active ligands, proton-responsive moieties, and secondary-sphere functionalities (such as intramolecular base sites or hydrogen-bond donors).[30,63] Such cooperative effects are

Table 1 Quantitative catalytic descriptors for optimizing the HER and OER

Parameter	Definition	HER (acidic/alkaline)	OER (acidic/alkaline)	Overall EWS
Thermodynamic potential (E°)	Minimum equilibrium potential under standard conditions (298 K, pH 0)	0.00 V (*vs.* RHE)	+1.23 V (*vs.* RHE)	1.23 V total
Overpotential (η)	Additional voltage required beyond E° to drive catalysis	<100 mV (target)	<400 mV (target)	Combined, system-dependent
Binding free energy (ΔG)	Optimal adsorption energy of key intermediates	$\Delta G_H \approx 0.0$ eV	ΔG_{OH}, ΔG_O, $\Delta G_{OOH} \approx$ 1.23 eV per step	Reflected in cumulative performance
Tafel slope	Kinetic indicator of rate-determining step	<60 mV dec^{-1}	<60 mV dec^{-1}	Aggregate from half-reactions
Exchange current density (j_0)	Intrinsic catalytic activity at zero overpotential	$\geq 10^{-3}$ A cm^{-2}	$\geq 10^{-5}$ A cm^{-2}	Determined by the slowest step
Turnover frequency (TOF)	Catalytic cycles per active site per second	>10 s^{-1}	>1 s^{-1}	Limited by OER kinetics
Turnover number (TON)	Total cycles before catalyst deactivation	>10^4	>10^4	Reflects long-term durability
Faradaic efficiency (FE)	Fraction of charge converted to target product	>95%	>95%	>95% overall
Reorganization energy (λ)	Energy cost of geometric and solvation rearrangements in PCET	Low (favors rapid PCET)	Low (favors redox turnover)	Co-optimized across both
d-Band center (electronic descriptor)	Correlates metal electronic structure to adsorbate binding strength	Tuned for balanced H* adsorption	Tuned for balanced OH*/O*/OOH* adsorption	Critical for bifunctional design
H_2/O_2 production rate	Volume or molar rate of gas generated per unit time and area	$\geq$10 mmol cm^{-2} h^{-1} (H_2)	$\geq$5 mmol cm^{-2} h^{-1} (O_2)	Stoichiometric ratio 2 : 1 (H_2 : O_2)
pH-Dependent potential shift	Theoretical shift per pH unit (Nernst equation)	~59 mV pH^{-1} unit	~59 mV pH^{-1} unit	Overall splitting remains invariant

often linked to low Tafel slopes in both systems and high TOFs in both half-reactions. To overcome the limitations of mononuclear systems, researchers have explored multi-nuclear complexes where cooperative metal centers modulate electron density and distribute oxidative stress across the framework. This design improves both catalytic activity and durability under bifunctional conditions.[37]

In parallel, hybrid frameworks that incorporate molecular catalysts into conductive or porous supports offer synergistic advantages. High surface area matrices such as carbon nanotubes, graphene, or mesoporous scaffolds improve mass transport, enhance electrochemical active surface area, and facilitate electron transfer across active sites.[64] In this regard, emerging materials that integrate MOF-derived active centers with molecular catalysts have demonstrated exceptional bifunctional performance. These systems benefits from modular coordination environments, high porosity, and strong metal–ligand covalency that collectively support both HER and OER.[41] Such hybridization enables tuning of local electric fields, improves electrolyte ion access, and prevents deactivation *via* leaching or ligand degradation. Effective bifunctional electrocatalysts must therefore combine redox flexibility, structural logic, interfacial stability, and vibrant proton–electron association within a single catalytic framework.[14,65] Rather than being separately optimized for each half-reaction, true bifunctionality arises from the integrated control of these interdependent properties at the molecular and mesoscale levels.

2.9. Illuminating the active state: real-time spectroscopic insights into metal complex-based electrocatalysts

The HER/OER process of EWS involves dynamic structural and electronic changes that essentially determine the durability and activity of the catalyst. These modifications, which are not detectable by traditional *ex situ* characterisation, frequently entail redox transitions, intermediate binding, and ligand rearrangements for Earth-abundant metal complexes. Thus, real-time spectro-electrochemical methods, which are conducted under applied potentials are essential for revealing the catalyst's active state, outlining mechanistic pathways, and confirming theoretical predictions.[66,67] One of the most effective methods for tracking metal oxidation states and local coordination environments during catalysis is X-ray absorption spectroscopy (XAS), which includes X-ray absorption near-edge structure (XANES) and extended X-ray absorption fine structure (EXAFS). In particular, valence transitions to Fe(IV) under anodic conditions have been found by operando XAS of Fe and Ni K-edges in Ni–Fe layered double hydroxides, suggesting the formation of catalytically relevant metal–oxo species during the OER.[68] Redox-induced Co(II)/Co(III)/Co(IV) transformations have also been shown by cobalt macrocyclic complexes under water oxidation conditions, suggesting the need for metal center's with multielectron processing capabilities.[69]

For monitoring ligand field shifts and electronic transitions in molecular complexes like phthalocyanines and porphyrins, *in situ* ultraviolet-visible (UV–Vis) spectroscopy is promising.[70] The development of catalytically active oxidation states or intermediates can be identified by changes in absorption profiles under an applied voltage. In addition, vibrational fingerprints of surface-bound species like M–OH, M=O, and bridging oxygen ligands can be obtained using infrared (IR) spectroscopy, particularly in the attenuated total reflectance (ATR) configuration.[71] These vibrational characteristics are important for differentiating between concerted and stepwise reaction pathways, and provide information on PCET activities during the HER and OER. Additional sensitivity to dynamic bonding environments and intermediate formation is provided by Raman spectroscopy, which includes resonance Raman and surface-enhanced Raman spectroscopy (SERS). As an instance, the time-resolved Raman technique has been used to track the O–O bond formation step in the OER *via* transient *OOH and *O vibrational modes in MOFs.[72] Nanogram-level mass changes at the electrode surface during catalytic turnover are monitored using an electrochemical quartz crystal microbalance (EQCM). This method has directly linked structural stability to operational durability by the identification of the mass increase brought about by hydroxide or oxide formation during the OER and mass loss brought about by ligand degradation or metal leaching.[73]

The study of surface oxidation states, coordination changes, and chemical composition under reaction-relevant conditions has benefited greatly from the use of near-ambient pressure X-ray photoelectron spectroscopy (AP-XPS). AP-XPS can reveal oxidation-induced ligand transformation under bias and distinguish surface-anchored $M–N_4$ sites from adsorbed hydroxide species for metal complexes anchored on conductive supports.[74] Kelvin probe force microscopy (KPFM) and scanning electrochemical microscopy (SECM) are spatially resolved methods for the mapping of electronic work function and local reactivity, respectively. While KPFM resolves potential gradients and local dipoles across hybrid catalyst interfaces, SECM enables imaging of active site density and proton reduction zones during the HER.[75] These observations are especially pertinent to heterogenized metal complexes, where surface coverage and redox gradients affect bifunctionality. Furthermore, product quantification and intermediate tracking have been made possible by new methods like electrochemical gas chromatography and differential electrochemical mass spectrometry (DEMS).[76] These data are helpful for verifying reaction selectivity and FE in intricate catalytic systems.

When combined, these real-time analytical tools have made it possible to directly correlate important electrochemical parameters like the TOF, exchange current density, Tafel slope, and overpotential with spectroscopic observables. Additionally, the direct detection of intermediates and active site motifs have made it possible to validate DFT predictions. Incorporation of these methods will become more and more essential as the field shifts toward logical, mechanism-driven catalyst development. Real-time characterization offers the mechanistic foundation for well-informed catalyst design in molecular and hybrid electrocatalysts, where minor modifications to the ligand environment or nuclearity can significantly alter the performance.

3. Catalytic innovations in earth-abundant metal complexes for dual-function electrochemical water splitting

Innovations in molecular electrocatalysts focusing on dual-functional systems that are capable of driving both the HER and OER have shown significant advancements. By emphasizing on catalytic strategies, mechanistic insights, and performance trends, this section highlights notable research breakthroughs achieved over the past decade. Among these molecular catalyst platforms, Aijian Wang and co-authors synthesized a cobalt-porphyrin-based covalent organic polymer (CoCOP) *via* Schiff-base condensation between 5,10,15,20-tetrakis(4-aminophenyl)-porphyrin (TPP) and 2-hydroxyterephthalaldehyde at 150 °C under a nitrogen atmosphere for 7 days, followed by cobalt incorporation through ultrasonication with $CoCl_2$ in DMF at 120 °C for 24 hours. Electrochemical evaluation of Co embedded CoCOP on carbon fiber paper (CFP) in 1.0 M KOH revealed low overpotentials of −310 mV (HER) and 350 mV (OER) at 10 mA cm^{-2}, with Tafel slopes of 161 and 151 mV dec^{-1}, respectively, and operational stability up to 7000 seconds. The Co-based active sites achieved TOF values of 0.024 s^{-1} (HER) and 0.013 s^{-1} (OER), supported by a high Brunauer–Emmett–Teller (BET) surface area of 289 m^2 g^{-1}, an electrochemical active surface area (ECSA) of 9.4 mF cm^{-2}, and low charge-transfer resistance, collectively enhancing active site accessibility, electron transfer, and overall catalytic performance.[77] Furthermore, Anindita Goswami *et al.* reported a simple *in situ* solvothermal method to fabricate a self-supported, binder-free Mn(II)–MOF electrode directly on nickel foam (Mn–MOF/NF). The material exhibited excellent bifunctional activity, achieving ultra-low overpotentials of 280 mV at 20 mA cm^{-2} for the OER and −125 mV at 10 mA cm^{-2} for the HER in 0.1 M KOH, with Tafel slopes of 80 mV dec^{-1} and 113 mV dec^{-1}, respectively. In a two-electrode setup, Mn–MOF/NF required only 1.68 V to reach 10 mA cm^{-2}, showing strong durability over prolonged cycling. Electrochemical analysis revealed a higher ECSA (261.34 cm^2) and C_{dl} (3.92 mF) compared to bare NF, alongside a notable roughness factor (261.34) and TOF (65.56 s^{-1}). The enhanced performance was attributed to the bimetallic synergy between Mn^{2+} and redox-active Ni^{2+} introduced from the self-sacrificial NF substrate, which provided improved electron transport, abundant active sites, and excellent electrolyte contact. Fig. 5 provides further details on the proposed OER and HER mechanisms, highlighting the key catalytic pathways involved at Mn–MOF/NF.[78]

Recently, Hongxin Guan *et al.* synthesized FeMn bimetallic MOFs on nickel foam (FeMn–MOF/NF) *via* a one-step solvo-

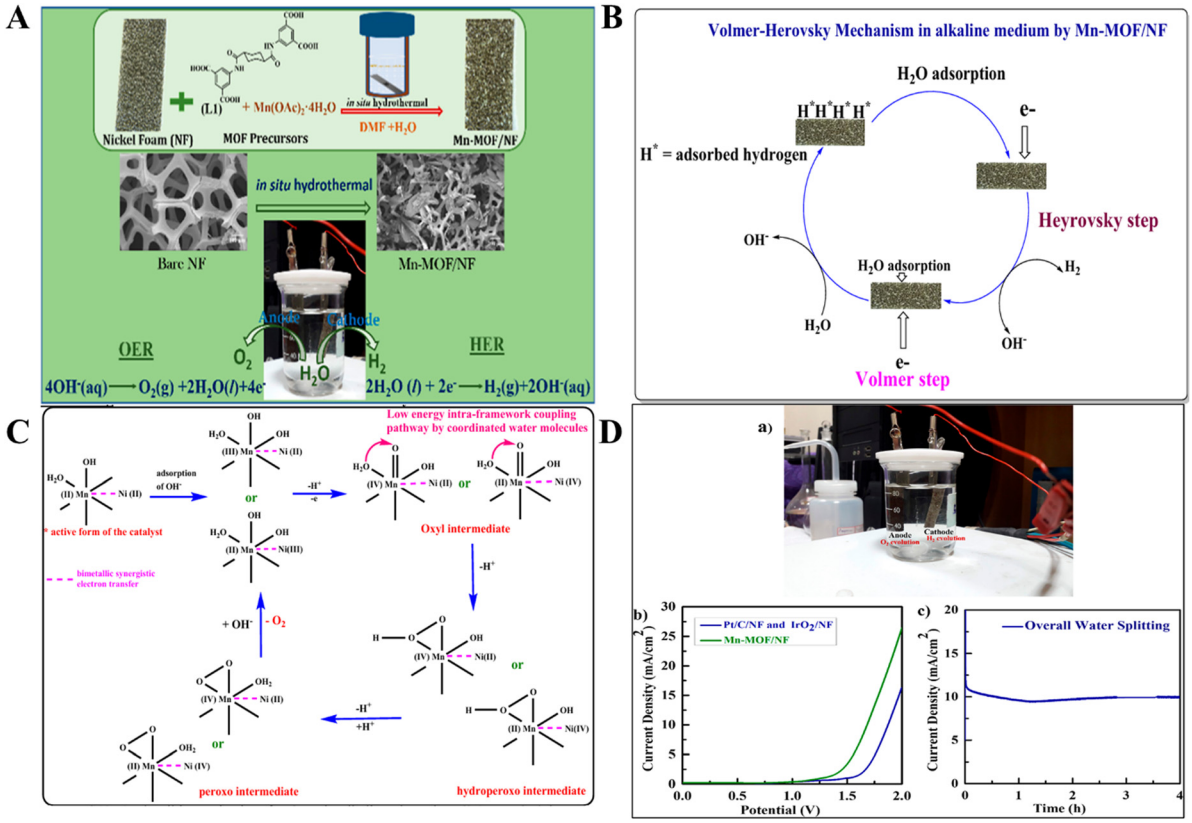

Fig. 5 (A) Schematic of Mn–MOF/NF electrocatalyst development; (B) proposed HER mechanism in 0.1 M KOH; (C) proposed OER mechanism in 0.1 M KOH; (D) overall EWS performance: (a) two-electrode setup photograph, (b) LSV polarization curve, and (c) long-term durability test [reproduced from ref. 78 with permission from the American Chemical Society, copyright 2022].

thermal method and constructed binder-free electrodes for overall EWS. The optimal Fe : Mn (1 : 1) system exhibited excellent bifunctional activity, achieving an OER overpotential of 290 mV and a HER overpotential of −260 mV at 50 mA cm^{-2}, with Tafel slopes of 87 mV dec^{-1} (OER) and 156.6 mV dec^{-1} (HER). It showed the highest C_{dl} (~3.66 mF cm^{-2}) among the tested variants and retained strong stability over 12 h with minimal performance loss after 1000 cycles. In a two-electrode setup, FeMn–MOF/NF required only 1.70 V at 50 mA cm^{-2} for overall water splitting, with just a ~0.02 V increase after 60 days. The outstanding activity was attributed to the Fe/Mn synergistic redox effects, high surface area from the 3D nanoflower morphology, and conductive NF support ensuring efficient charge transfer.[79] Furthermore, Liu *et al.* synthesized two-dimensional CoNi–metal–organic framework (CoNi–MOF) nanoplate arrays on Cu foil through a hydrothermal method, demonstrating excellent catalytic performance for alkaline water splitting. The optimized Co : Ni (1 : 1) MOF displayed dominant (220) facets, providing enhanced conductivity along the *Z*-axis and abundant exposed active sites. In 1.0 M KOH, the CoNi (1 : 1)–MOF achieved an overpotential of 265 mV at 10 mA cm^{-2} for the OER, with a low Tafel slope of 56 mV dec^{-1} and minimal charge-transfer resistance (0.924 Ω), outperforming single-metal MOFs and RuO_2. The catalyst maintained ~90% activity over 20 hours. After annealing under NH_3, the CoNiN@C hybrid, consisting of metallic nitrides on a porous carbon framework, delivered an efficient HER, requiring only a −120 mV overpotential at 10 mA cm^{-2}, with improved capacitance (39.2 mF cm^{-2}) and lower charge-transfer resistance (4.62 Ω). In a two-electrode setup, combining CoNi(1 : 1)–MOF and CoNiN@C achieved overall water splitting at 1.64 V with ~99% FE, confirming the designed system's high bifunctional catalytic activity.[80] Using the pyrolysis of dual-ligand Co–MOFs assembled from thiophene-2,5-dicarboxylate and 4,4′-bipyridine on graphene oxide at 1000 °C, Zhang *et al.* developed a bifunctional electrocatalyst composed of Co/Co_9S_8 core–shell nanoparticles embedded in S,N-doped porous graphene sheets (Co/Co_9S_8@SNGS). The resultant hybrid endured uniform heteroatom doping, hierarchical porosity, and a high surface area (249.6 m^2 g^{-1}). Excellent bifunctional activity was demonstrated by electrochemical studies in 0.1 M KOH, with an OER overpotential of 290 mV at 10 mA cm^{-2} (Tafel slope: 73 mV dec^{-1}) and a HER overpotential of 350 mV at 20 mA cm^{-2} (Tafel slope: 96 mV dec^{-1}). With nearly 100% FE, full EWS with identical electrodes produced H_2 and O_2 evolution rates of 4.87 and 2.48 μmol min^{-1}, respectively, at 1.58 V. Synergistic effects between the metallic Co core, Co_9S_8 shell, S,N co-doping, and Co–N_x sites are responsible for the enhanced performance. These effects jointly boost conductivity, accessibility of the active sites, and catalytic durability. The potential benefit of dual-heteroatom MOF precursors in designing integrated electrocatalysts for general alkaline water electrolysis is demonstrated in this work.[81]

Basically, Ni and Fe bimetallic complexes are highly promising electrocatalysts for bifunctional water splitting reactions. Duan *et al.* developed ultrathin 2D NiFe–MOF nanosheet arrays *via* a one-step chemical bath deposition using 2,6-naphthalenedicarboxylic acid dipotassium (NDCA) as the organic linker with Ni and Fe salts. The crystalline structure, built from alternating NDCA units and octahedral MO_6 (M = Ni, Fe) directly grown on nickel foam (NF), forms meso- and macro-porous architectures. In 0.1 M KOH, NiFe–MOF/NF showed excellent OER activity, requiring only a 240 mV overpotential at 10 mA cm^{-2}, outperforming the Ni–MOF (296 mV), Fe–MOF (324 mV), and NiFe–MOF on glassy carbon (406 mV). For the HER, the NiFe–MOF achieved an overpotential of −134 mV at 10 mA cm^{-2}, superior to those of the Ni–MOF (−177 mV), bulk NiFe–MOF (−196 mV), and calcined NiFe–MOF (−255 mV). Stability testing confirmed consistent HER and OER activity over 20 000 s. As a full water-splitting cell, the NiFe–MOF used as both electrodes delivered 10 mA cm^{-2} at 1.55 V for 20 h without notable activity loss (Fig. 6). The enhanced catalytic performance arises from the nanosheet architecture exposing abundant Ni/Fe active sites, improving conductivity, and enabling efficient mass transport. However, only one Fe composition (23%) was studied, leaving room for future optimization.[82] Using mild heat, Lin *et al.* phosphated Fe/Ni-based MOF-derived nanosheet arrays on nickel foam to create the bifunctional electrocatalyst $(Fe_{0.1}Ni_{0.9})_2P(O)$/NF. Ni, Fe, P, and O were uniformly distributed in the final material. The addition of Fe caused lattice distortion, while the addition of oxygen contributed to altered surface chemistry. An overpotential of 240 mV at 100 mA cm^{-2} for the OER with a Tafel slope of 72 mV dec^{-1} and 87 mV at 10 mA cm^{-2} for the HER with stable kinetics were noticed from electrochemical measurements in 1.0 M KOH, which demonstrated efficient activity for both half-reactions. The system demonstrated approximately 100% FE, maintained current stability for 40 hours, and required 1.50 V to sustain 10 mA cm^{-2} when used as both the anode and cathode in a two-electrode setup. Fe–Ni interactions, high electrochemical active surface area, oxygen doping, and decreased charge-transfer resistance from the precursor transformation process were all associated with the boosting of performance.[83]

Furthermore, Yang *et al.* developed the bifunctional NF@FePPc-s/p catalyst by phosphidating surfactant-modified iron polyphthalocyanine grown on nickel foam, producing Fe_2P and Ni_2P phases with a unique needle mushroom-like morphology. In 1.0 M KOH, it achieved low overpotentials of −190 mV (HER) and 293 mV (OER) at 100 mA cm^{-2}, with Tafel slopes of 123.1 and 82.4 mV dec^{-1}, respectively, outperforming NF@Pt/C and NF@RuO_2 references. The catalyst showed the highest ECSA (C_{dl}: ~43 mF cm^{-2}) and low charge transfer resistance (3.3 Ω), indicating abundant active sites and fast kinetics. Faradaic efficiencies reached ~95% for H_2 and ~96% for O_2. Long-term tests showed minimal overpotential shifts after 5000–15 000 cycles, with ~96–98% current retention over 24 h. In a full water-splitting cell, NF@FePPc-s/p‖NF@FePPc-s/p required only 1.433 V at 10 mA cm^{-2} and 1.743 V at 100 mA cm^{-2}, surpassing Pt/C‖RuO_2 benchmarks, with post-cycling XPS confirming Fe_2P-to-FeOOH conversion (OER) and stable Fe_2P (HER).[84] Similarly, Qiuxiang Mou's group developed a

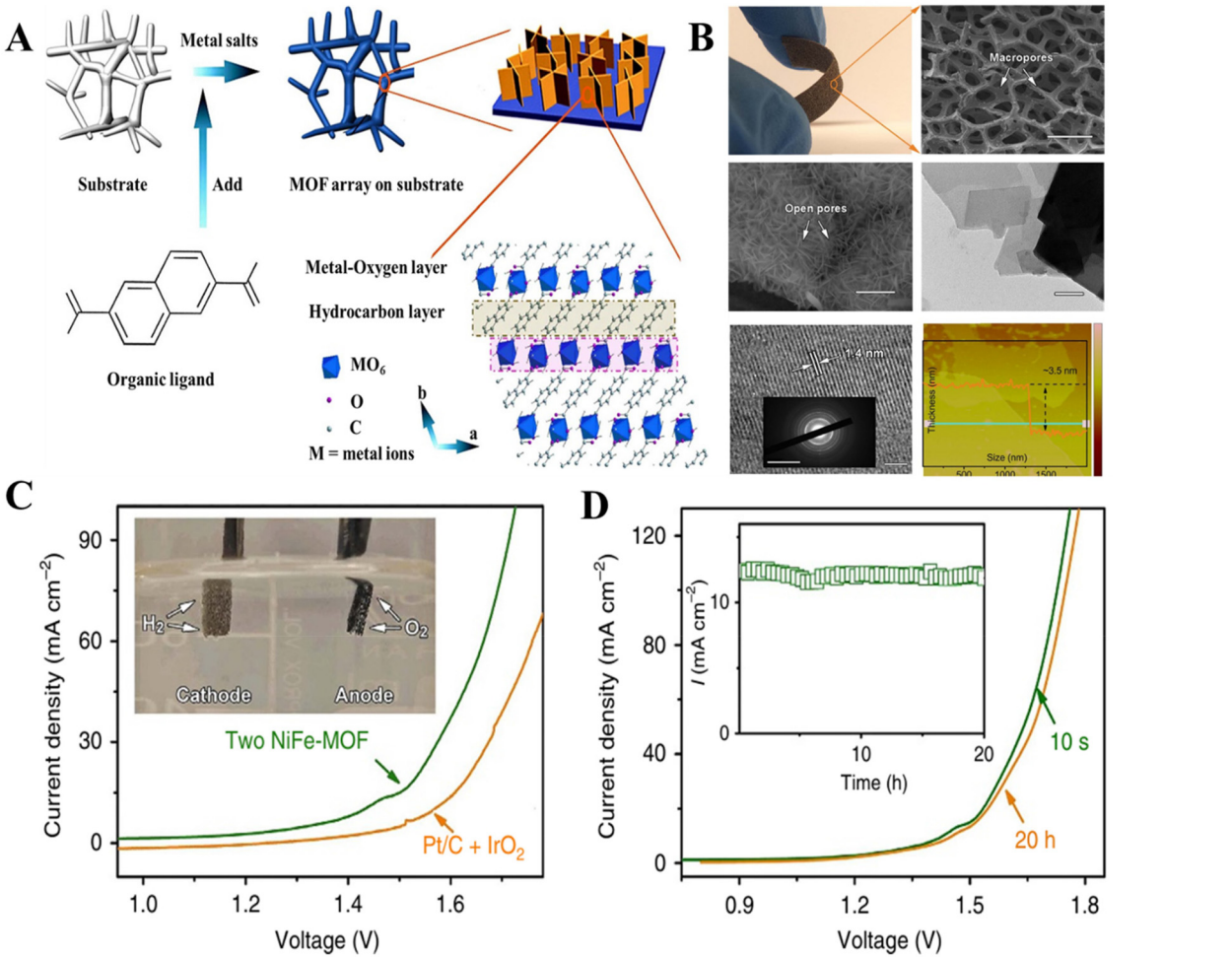

Fig. 6 (A) Schematic of NiFe–MOF nanosheet array synthesis; (B) morphological characterization: optical, SEM, TEM, HRTEM, SAED, and AFM images; (C) LSV plots of a two-electrode cell with NiFe–MOF electrodes in 0.1 M KOH, including comparison with Pt/C||IrO_2 and gas bubble evolution at 1.6 V; (D) LSV before and after 20 h chronoamperometric testing at 1.5 V, with the inset showing a stability plot [reproduced from ref. 82 under the terms of the Creative Commons Attribution 4.0 International License (CC BY 4.0)].

NiFe–MOF-5 catalyst with a 3D hierarchical structure grown on Ni foam *via* a one-step solvothermal method. Nickel(II) nitrate, iron(III) nitrate, and formic acid were dissolved in DMF, and Ni foam was immersed and heated at 100 °C for 12 h in a sealed autoclave. NiFe–MOF-5 exhibited excellent bifunctional activity, with overpotentials of −163 mV (HER) and 168 mV (OER) at 10 mA cm^{-2}, and Tafel slopes of 139 mV dec^{-1} (HER) and 43 mV dec^{-1} (OER), indicating fast kinetics. Overall water splitting required just 1.57 V at 10 mA cm^{-2} in 1.0 M KOH, outperforming many non-precious catalysts, with stable performance maintained over 24 h at 1.8 V and 10 000 LSV cycles.[85]

Trimetallic MOFs containing Fe, Ni and Co act as efficient multifunctional catalysts. For instance, Farahani *et al.* developed an innovative and tunable electrodeposition method for *in situ* growth of a trimetallic Fe–Co–Ni MOF on nickel foam using a layer-by-layer (LbL) reductive approach. This process was carried out in a DMF/H_2O solution with metal ions, cetyltrimethylammonium bromide (CTAB), and 2-amino-1,4-benzenedicarboxylic acid yielding a distinct trilayer MOF structure, confirmed by cross-sectional SEM results. In 1.0 M KOH, the Fe–Co–Ni MOF achieved an overpotential of 254 mV at 10 mA cm^{-2} for OER, outperforming the Fe–Co MOF (280 mV), Fe MOF (290 mV), and bare Ni foam (440 mV), with a Tafel slope of 51.3 mV dec^{-1} and stability up to 48 h. HER activity followed the same trend, and a two-electrode cell required only 1.6 V at 10 mA cm^{-2}, maintaining stability for 150 h, surpassing Pt/C||RuO_2 (1.62 V). Post-stability XPS revealed a slight increase in trivalent species, indicating possible (oxy)hydroxide formation. DFT calculations showed that the Fe–Co–Ni MOF had more negative H_2O adsorption energy, a smaller bandgap, and higher electronic density near the Fermi level compared to mono- and bimetallic MOFs, enhancing conductivity and catalytic performance. Notably, the material also exhibited excellent ORR activity, making it suitable for Zn–air batteries and supercapacitors.[86] Besides pyrolyzing MOF precursors, complex metal compounds with varied nanostructures and compositions were also synthesized, serving as efficient bifunctional electrocatalysts for both the HER and OER.[87] For

instance, Das *et al.* developed Ni/Mo_xC–NC, combining nickel and molybdenum carbide nanoparticles on nitrogen-doped graphene/carbon nanotube supports, through thermal treatment of $NiMoO_4{\cdot}xH_2O$ and melamine at 850 °C under nitrogen. TEM and HR-TEM confirmed the presence of Mo_2C, MoC, and Ni crystalline phases embedded in the carbon matrix. In 1.0 M KOH, Ni/Mo_xC–NC showed excellent HER and OER performance, with overpotentials of −162 mV and 328 mV at 10 mA cm^{-2}, Tafel slopes of 104 and 74 mV dec^{-1}, and the highest ECSA (29.8 mF cm^{-2}) among the tested catalysts. The system achieved overall water splitting at 1.72 V, comparable to that of Pt/C||RuO_2, and generated H_2 and O_2 at 0.034 and 0.0165 mL min^{-1} (Fig. 7). Mechanistic analysis showed that Ni^{2+} species promote water dissociation (Volmer step), MoC provides Pt-like electronic features, and pyridinic–N enriches the carbon surface, increasing catalytic sites. For the OER, the transformation of Ni(II) to NiOOH plays a key role, with the system delivering better performance and a shifted oxidation peak compared to Ni/NC-100.[88]

Apart from molecularly defined metal complexes, a lot of recent catalyst structures use materials derived from MOFs. In these materials, Earth-abundant metal frameworks, like ZIF-67, act as both structural scaffolds and metal avenues and, undergo regulated post-synthetic morphing to produce highly active electrocatalysts. These systems, which frequently combine the robustness and conductivity of metal phosphides, nitrides, or oxides with the creative tunability of molecular precursors, fill the void between homogeneous molecular catalysts and heterogeneous nanostructures. For instance, Li *et al.* developed ultrathin Mn-doped CoP nanosheets (Mn–CoP) using an etching-carbonization–phosphidation method starting from rhombic dodecahedral ZIF-67 precursors. These Mn–CoP nanosheets exhibited remarkable bifunctional electrocatalytic performance for the HER and OER, achieving overpotentials of −148 mV (acidic) and −195 mV (alkaline) for the HER, and 290 mV (alkaline) for the OER at 10 mA cm^{-2}, outperforming hollow CoP and Mn–CoP nanoparticles, and even commercial RuO_2. The materials showed Tafel slopes of 61 and 85 mV dec^{-1} (HER) and 76 mV dec^{-1} (OER), alongside excellent long-term durability up to 30 h. Structural analysis confirmed a large BET surface area (357.7 m^2 g^{-1}), meso-porosity, and uniform distribution of Mn, Co, P, C, and N. Electrochemical impedance spectroscopy revealed low charge-transfer resistance (R_{ct} ~30 Ω acidic, ~35 Ω alkaline for the HER; ~20 Ω for the OER), and the double-layer capacitance (C_{dl}) reached 21.1 mF cm^{-2}, indicating a high electrochemical active surface area. XPS analysis showed Mn^{2+}/Mn^{4+} states and Co–P bonding, while N-doping enhanced electronic conductivity and optimized the adsorption energies.[89]

Likewise, Xia Shi and co-workers developed Co–Mo_2N hollow tube catalysts using a "MOFs plus MOFs" strategy for alkaline (1.0 M KOH) water splitting. One-dimensional Mo–MOFs were first synthesized by reacting imidazole with MoO_3, and then coated with ZIF-67 (Co source) *via* solution-phase assembly, leveraging their ligand compatibility. Upon nitridation, ZIF-67 converted to metallic Co and Mo–MOFs converted

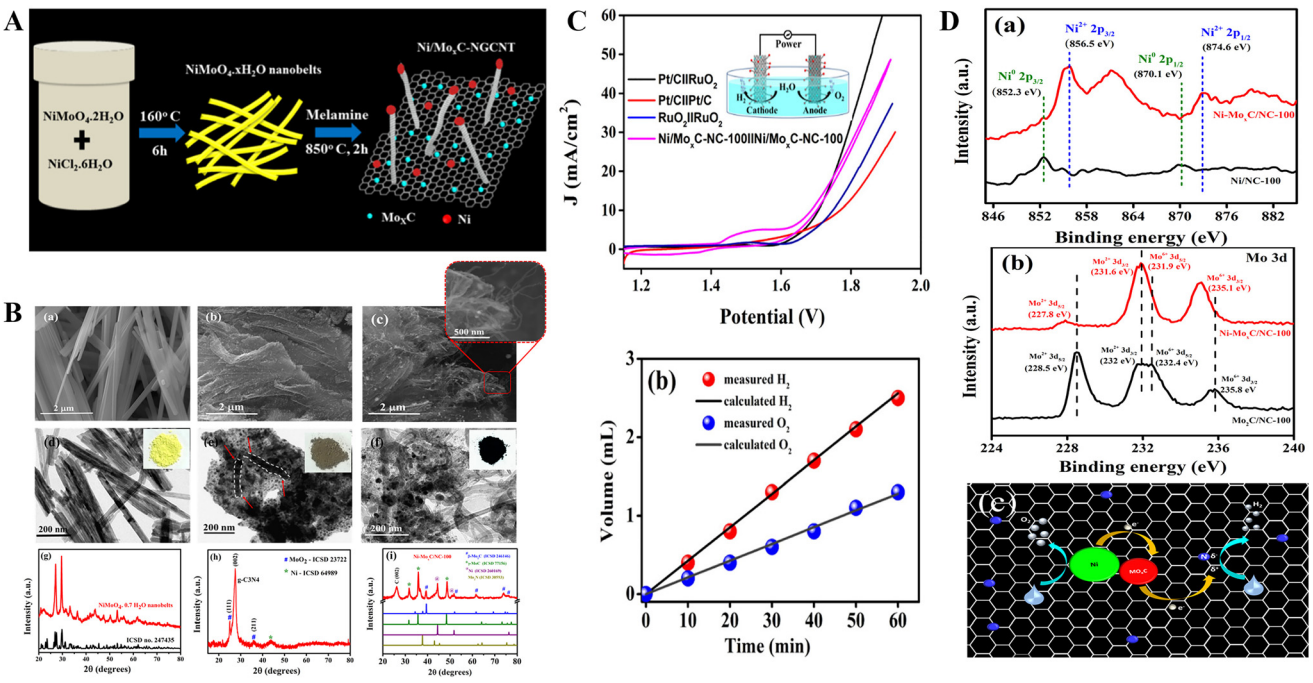

Fig. 7 (A) Schematic of Ni/MoxC–NC synthesis; (B) FESEM, TEM, and XRD of $NiMoO_4{\cdot}0.7H_2O$ nanobelts, Ni/MoO_2–gC_3N_4 sheets, and Ni/MoxC–NC; (C) (a) polarization curves for overall water splitting in 1.0 M KOH, (b) H_2 and O_2 production over time; (D) (a and b) high-resolution XPS spectra (Ni 2p, Mo 3d), and (c) schematic of electron transfer pathways in water splitting [reproduced from ref. 88 with permission from the American Chemical Society, copyright 2018].

to hollow Mo_2N and, formed a Co–Mo_2N hybrid with a tunable Co/Mo ratio. SEM and TEM confirmed rod-shaped Mo–MOFs decorated with ZIF-67 polyhedrons, while BET analysis showed a high surface area (~1143 m^2 g^{-1}). Electrochemical tests revealed excellent HER performance with an overpotential of −76 mV at 10 mA cm^{-2}, a Tafel slope of 47 mV dec^{-1}, an exchange current density of −0.52 mA cm^{-2}, a TOF of 0.396 s^{-1}, and a FE of 100%. For the OER, the catalyst required 302 mV at 10 mA cm^{-2} with a Tafel slope of 90 mV dec^{-1} and an ECSA of 42.8 mF cm^{-2}, and maintained stability for 48 h (HER) and 24 h (OER). A two-electrode Co–Mo_2N||Co–Mo_2N system delivered overall water splitting at 1.576 V with 40 h stability (Fig. 8). DFT and XPS data indicated that electron-rich Mo optimizes H adsorption (ΔG^* near zero), and late transition metals (LTMs) modulate Mo_2N's electronic structure to further lower ΔG^*. The hollow, rough-surfaced architecture increases active site exposure and promotes gas release, while Mo_2N's excellent conductivity enables fast electron transfer. Scanning Kelvin Probe (SKP) measurements confirmed a work function of 5.56 eV, comparable to that of Pt (5.60 eV), supporting its high catalytic potential.[90] Similarly, Jianrui Sun *et al.* synthesized trimetallic Fe/Ni/Co phosphides (FeCoNiP@NC) *via* a crystallization method using ZIF-67/GO precursors, forming heterojunctions between FeP, CoP, and Ni_2P supported on graphene. Structural analyses (XRD, SEM, TEM, and XPS) confirmed well-dispersed <10 nm phosphide nanoparticles. The catalyst achieved low HER overpotentials of −93 mV (0.5 M H_2SO_4) and −187 mV (1.0 M KOH), and an OER overpotential of 266 mV (1.0 M KOH) at 10 mA cm^{-2}. A FeCoNiP@NC/Ni two-electrode system delivered 10 mA cm^{-2} at 1.73 V for overall water splitting with good 10 h stability. The combined roles of FeP and CoP enhanced the HER, while CoP mainly drove the OER, with graphene providing structural support and stability.[91]

Liang and co-workers developed bifunctional Co–NC@Mo_2C composites, where cobalt nanoparticles embedded in nitrogen-doped carbon (Co–NC) are reverse-encapsulated by molybdenum carbide (Mo_2C), forming a carbon-based framework with outstanding catalytic efficiency for overall EWS. The synthesis involved preparing ZIF-67 by mixing $Co(NO_3)_2{\cdot}6H_2O$ and 2-methylimidazole in methanol, followed by annealing with ammonium molybdate tetrahydrate at 700 °C under argon for 3 h. Structural characterization by XRD, XPS, and TEM confirmed the formation of a hollow, well-integrated composite, where the Mo_2C shell provides both protection against electrolyte corrosion and additional catalytic sites. In 1.0 M KOH, Co–NC@Mo_2C showed excellent HER and OER performance, with low overpotentials of −99 mV and 347 mV at 10 mA cm^{-2}, and Tafel slopes of 65 and 61 mV dec^{-1}, respectively. Impressively, it maintained good HER activity in acidic media (−143 mV at 10 mA cm^{-2}) and delivered an overall water-splitting cell voltage of just 1.685 V at 10 mA cm^{-2}, comparable to those of IrO_2–Pt/C systems, while retaining ~79% activity after 20 h (Fig. 9). Mechanistically, the intimate Co–Mo_2C interface facilitates charge transfer, improves intrinsic activity, and ensures long-term durability, demonstrating the promising potential of MOF-derived reverse-encapsulation strategies for designing efficient,

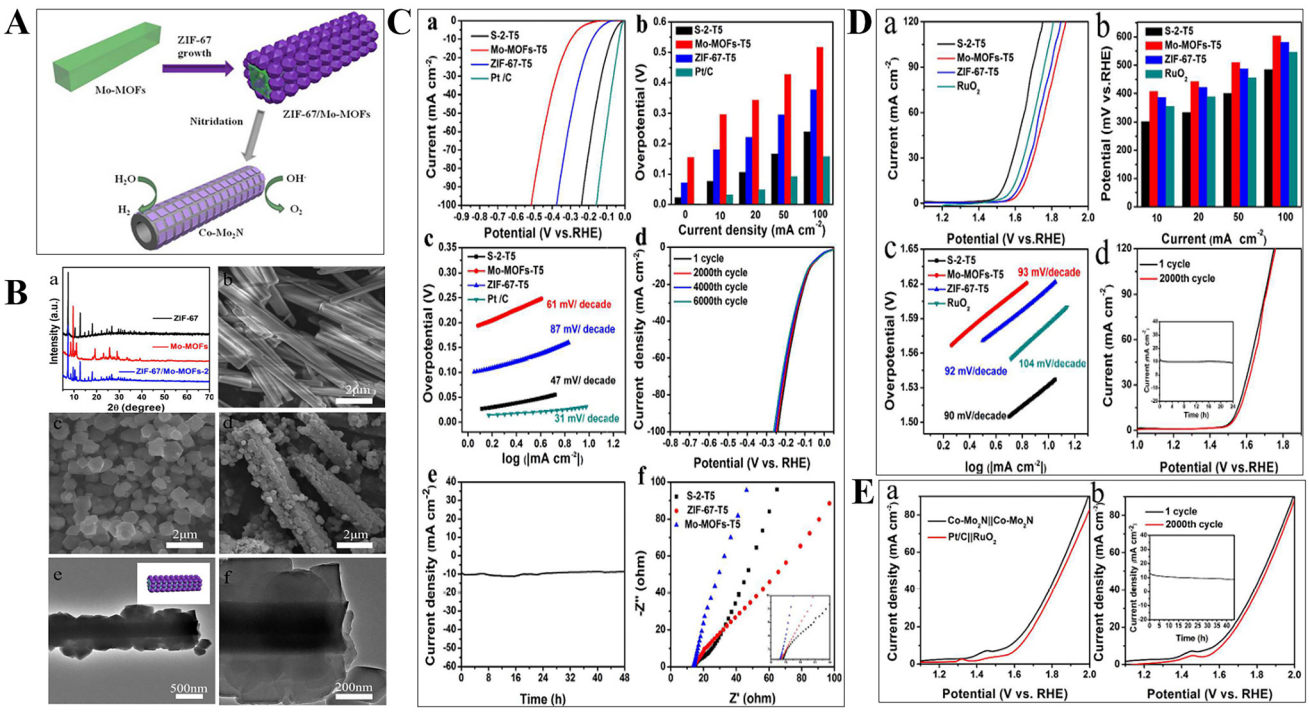

Fig. 8 (A) Schematic synthesis of a Co–Mo_2N hybrid; (B) XRD, SEM, and TEM of ZIF-67/Mo–MOFs; (C) HER performance: polarization, overpotentials, Tafel plots, stability, and EIS; (D) OER performance: LSV, overpotentials, Tafel plots, and durability; (E) overall water splitting: LSV, cycling, and long-term stability compared to those of Pt/C||RuO_2 [reproduced from ref. 90 with permission from the Royal Society of Chemistry].

non-precious bifunctional electrocatalysts.[92] Likewise, Pan *et al.* designed a bifunctional electrocatalyst consisting of cobalt phosphide (CoP) nanoparticles embedded within nitrogen-doped carbon nanotube hollow polyhedra (CoP/NCNHP), synthesized from a core–shell ZIF-8@ZIF-67 precursor through a controlled pyrolysis, oxidation, and phosphidation process. This unique architecture combines the high catalytic activity of CoP with the excellent conductivity and protective features of the porous N-doped carbon framework, creating abundant accessible active sites and facilitating efficient charge transfer. Electrochemical testing revealed outstanding performance, with overpotentials of −140 mV (HER, 0.5 M H_2SO_4), −115 mV (HER, 1.0 M KOH), and 310 mV (OER, 1.0 M KOH) at 10 mA cm^{-2}. The catalyst also achieved a low overall water-splitting cell voltage of 1.64 V, maintaining stable operation over 36 hours (Fig. 10). DFT calculations indicated that the N-doped carbon enhances Co d-orbital electron density, optimizing hydrogen adsorption for the HER, while the CoP/CoOOH interface plays a crucial role in OER activity. This work demonstrates the potential of MOF-derived hybrid materials for creating durable, high-performance bifunctional electrocatalysts.[93]

In addition, Wenxia Chen *et al.* reported a bifunctional CoPO/NF (cobalt hollow phosphorus polyhedral nanostructures on Ni foam) catalyst synthesized by transforming ZIF-67/Ni foam through high-temperature annealing, Ar–N_2 plasma treatment with a phosphorus precursor, and subsequent oxygen incorporation at lower temperatures. This process yielded a hollow, porous Co–P nanocage structure with a high surface area (BET: 1530 m^2 g^{-1}), abundant active sites (ECSA: 11.4 mF cm^{-2}, ~3.8 times higher than ZIF-67), and reduced charge-transfer resistance (18.8 Ω). In 1.0 M KOH, CoPO/NF exhibited excellent HER and OER performance, requiring overpotentials of only −105 mV and 275 mV at 10 mA cm^{-2}, with Tafel slopes of 48 and 52 mV dec^{-1}, respectively. The catalyst achieved H_2 and O_2 production rates of 1031 and 515 μmol h^{-1} with nearly 100% FE and demonstrated stable operation over 45 hours. DFT calculations indicated significant charge transfer from CoO to phosphorus, generating electron-rich P regions that enhanced water adsorption (−1.18 eV), raised the Fermi level, and produced an optimal hydrogen adsorption free energy ($\Delta G_{H^*} \approx 0$ eV) (Fig. 11). Post-reaction XPS analysis showed some oxidation of Co to Co_3O_4 and partial phosphorus loss, although the catalyst maintained its structural integrity and catalytic performance.[94]

Using a direct selenization route, Meng *et al.* fabricated a bifunctional catalyst ($Co_{0.85}Se$@NC) by thermally converting ZIF-67 into a composite of ultrafine $Co_{0.85}Se$ nanoparticles which are uniformly confined within a nitrogen-doped carbon matrix. The resulting material retained the parent MOF's poly-

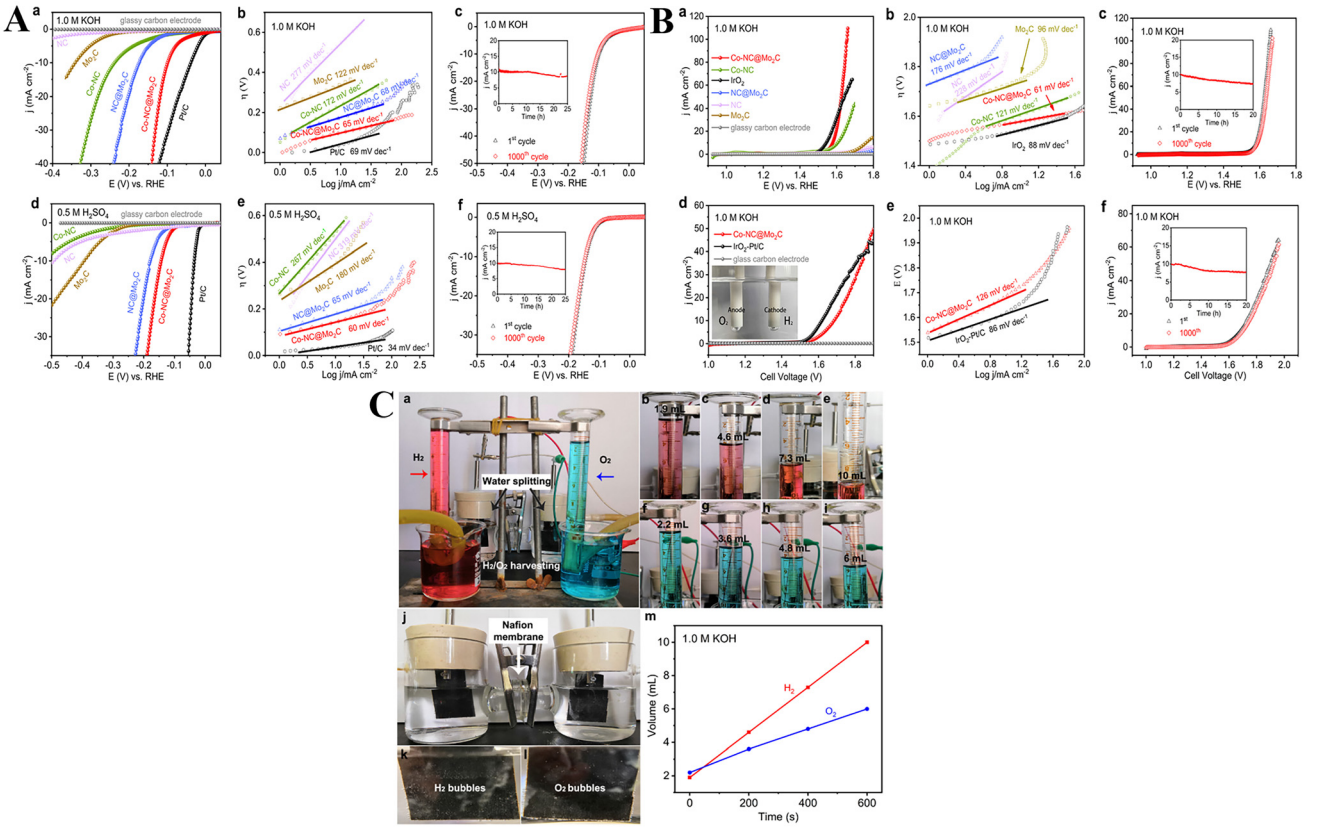

Fig. 9 (A) HER performance in 1.0 M KOH and 0.5 M H_2SO_4: polarization curves, Tafel plots, long-term stability, and cycling; (B) OER and overall water-splitting performance: polarization, Tafel curves, stability, and LSV; (C) gas collection setup and time-resolved measurements of H_2 and O_2 evolution in 1.0 M KOH, including device and bubble images, and quantified gas production over time [reproduced from ref. 92 with permission from Elsevier, copyright 2019].

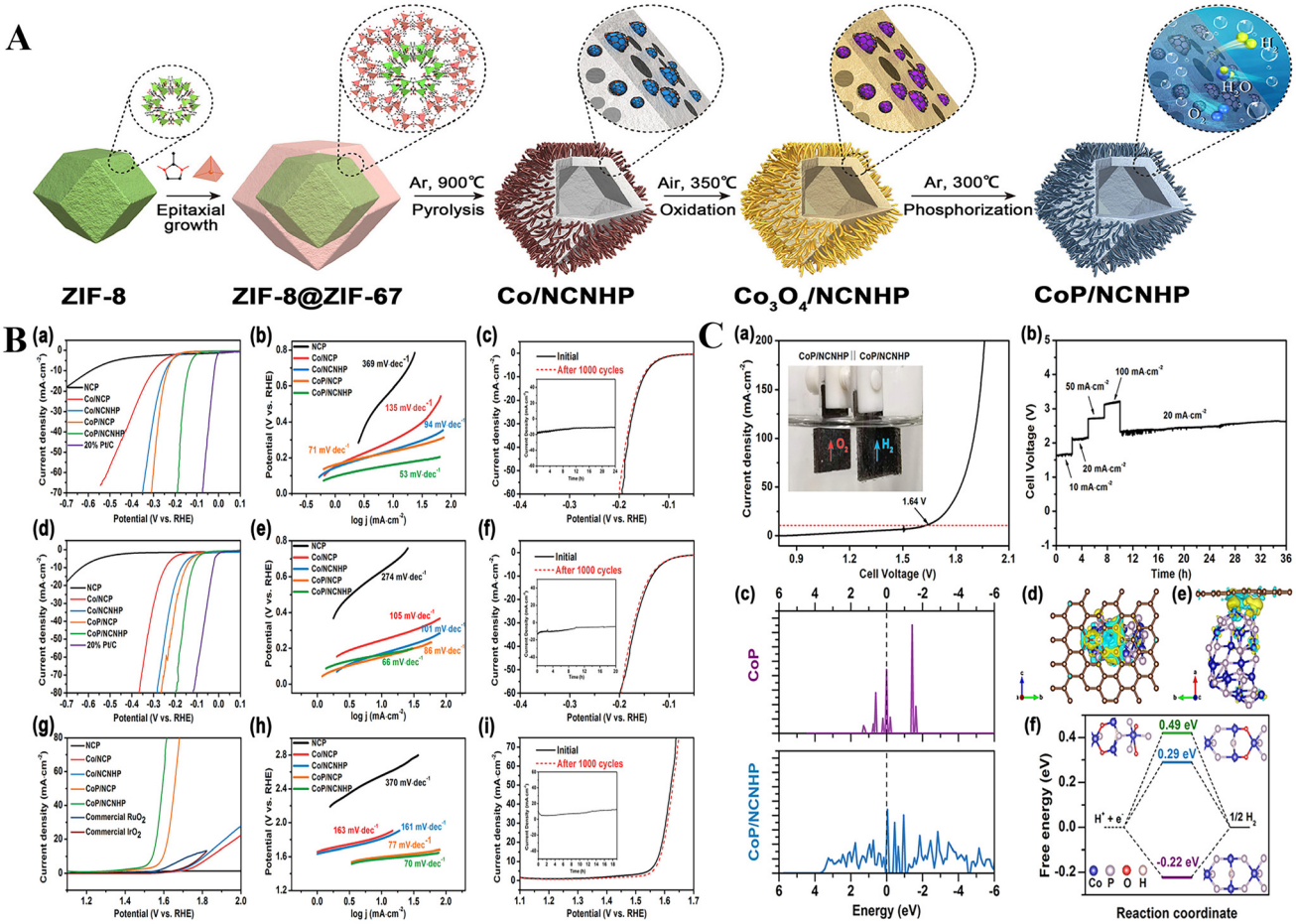

Fig. 10 (A) Schematic of CoP/NCNHP synthesis; (B) LSV, Tafel plots, and stability tests for the HER (0.5 M H_2SO_4, 1.0 M KOH) and OER (1.0 M KOH); (C) two-electrode water-splitting performance, chronopotentiometry, digital images of gas evolution, and DFT results including DOS, charge density, and HER free-energy diagrams [reproduced from ref. 93 with permission from the American Chemical Society, copyright 2018].

hedral geometry, developed hierarchical mesopores (2–20 nm), and achieved a surface area of 55 $m^2\ g^{-1}$. Structural analyses confirmed the formation of Co–N_x moieties, which played a key role in enhancing the catalytic activity. Electrochemical tests in alkaline medium (1.0 M KOH) showed excellent OER performance, with an onset potential of 1.49 V, a low overpotential of 320 mV at 10 mA cm^{-2}, and a Tafel slope of 75 mV dec^{-1}, along with a FE of 97.5% and long-term operational stability over 1000 cycles. In HER studies, the same material delivered an overpotential of −240 mV at 10 mA cm^{-2} and a Tafel slope of 135 mV dec^{-1}. When assembled into a symmetrical electrolyzer configuration, $Co_{0.85}Se$@NC required just 1.76 V to achieve 10 mA cm^{-2}, maintaining steady operation for 35 hours. The enhanced activity and durability were attributed to the synergistic interaction between nanoscale $Co_{0.85}Se$ and the conductive N-doped carbon framework, combined with high nitrogen incorporation (5.26 wt%) and electronic modulation through Co–N_x coordination.[95] Table 2 summarizes reported Earth-abundant metal (Mn, Fe, Co, Ni, and Mo) complexes and MOF-derived systems for the HER, OER, and bifunctional overall water splitting.

Furthermore, the integration of *in situ* spectroscopic tools reveals real-time structural dynamics under electrochemical conditions. In an impressive example, Jia *et al.* created a hybrid catalyst by decorating a cobalt-based metal–organic framework (Co–MOF-74) with cobalt phthalocyanine (CoPc), resulting in a composite known as Co–MOF-74@CoPc. The production of high-valent cobalt species, which are normally thermodynamically disfavoured under OER conditions, was greatly accelerated by this π-conjugated molecular modification technique. With a robust durability of over 210 hours in 1.0 M KOH and a low overpotential of 291 mV at 10 mA cm^{-2}, the resultant hybrid demonstrated exceptional electrocatalytic performance. Strong electronic coupling between CoPc and the Co–MOF scaffold was confirmed by XPS and XAS, with the former modifying the local coordination environment surrounding Co centers. Interestingly, *in situ* Raman spectroscopy showed that CoPc helped the MOF change into α-$Co(OH)_2$ at low potentials, which then changed into disordered CoOOH and $Co(IV)O_2$ species when anodic polarization occurred. Dynamic reconstruction and catalytic activity were directly correlated by spectroscopically confirmed structural transitions. This study emphasizes the crucial role of *in situ* spec-

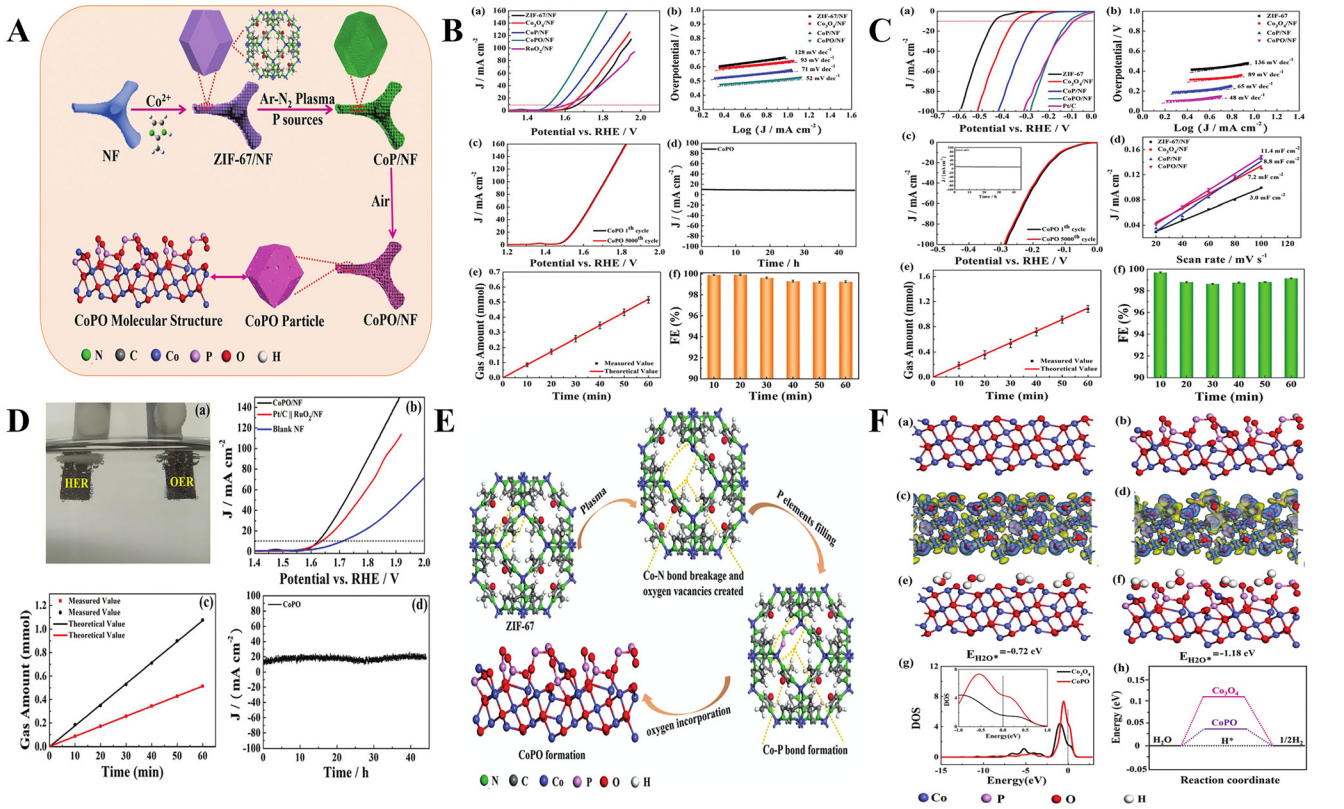

Fig. 11 (A) Synthesis of the CoPO/NF bifunctional electrocatalyst; (B) OER performance: polarization curves, Tafel slopes, stability, chronoamperometry, O_2 generation, and FE; (C) HER performance: polarization, Tafel slopes, stability, C_{dl} comparison, H_2 generation, and FE; (D) bifunctional water splitting: device setup, overall performance, gas evolution, and current stability; (E) formation mechanism of CoPO; (F) mechanistic insights from atomistic models: optimized structures, charge distributions, water adsorption energies, density of states, and HER free energy profiles [reproduced from ref. 94 with permission from the Royal Society of Chemistry].

troscopy in revealing real-time active-site evolution.[118] Similarly, Linke *et al.* used *in situ* XAS and XRD to study Ni–MOF-74 under electrochemical OER conditions, offering a complementary perspective on catalyst reconstruction. They discovered that during anodic polarization, Ni–MOF-74 experiences irreversible amorphization, resulting in the formation of an active NiOOH–metal organic phase (Ni–MOC*), which is responsible for the observed catalytic enhancement. A progressive oxidation of Ni centers identified by XAS and a loss of crystallinity in real-time XRD verified the transformation. Surprisingly, the reconstructed phase maintained operational stability for more than 100 hours at 500 mA cm^{-2} in an AEM electrolyzer and delivered a high current density of 14 A g Ni^{-1} at 1.5 V *vs.* RHE. This clear link between structural reorganization and electrochemical activation supports the usefulness of *in situ* spectroscopy in determining the functional states of MOF-based electrocatalysts and identifies amorphization as a feasible method for producing catalytically competent phases.[119]

A compelling extension of such *in situ* investigations was provided by Wu *et al.*, who developed a MOF-derived bifunctional electrocatalyst (C@NiCoP/NF) for efficient urea-assisted hydrogen production. A Ni–Co bimetallic phosphide composite (C@NiCoP/NF) with superior electrical conductivity and hierarchical porosity was produced by phosphidating ZIF-67 grown on nickel foam and then coating it with carbon. *In situ* spectroscopic investigations and DFT analyses verified the dynamic surface reconstruction of NiCoP into NiOOH and $Co(OH)_2$ during the urea oxidation reaction (UOR) and HER, forming the real catalytically active phase. In addition to increasing the electrochemical active surface area and improving the adsorption–desorption behaviour of urea-derived intermediates, the reconstructed surface also improved HER kinetics by optimizing H adsorption energies* and enhancing water molecule activation. With the catalyst requiring only 1.34 V to reach 100 mA cm^{-2} for the UOR and exhibiting a low HER overpotential of 168 mV at −100 mA cm^{-2}, the synergistic effects allowed for superior bifunctional performance. Compared to traditional OER-driven electrolysis, C@NiCoP/NF||C@NiCoP/NF required only 1.51 V to deliver 100 mA cm^{-2} in a full cell consisting of a urea-assisted water splitting setup. By highlighting the importance of electrochemical reconstruction as a catalyst design strategy in dual-function electrolyzers and offering mechanistic clarity into the operando formation of $NiOOH/Co(OH)_2$, this work emphasizes the significance of *in situ* spectroscopy in revealing transient phase transformations and active site evolution in MOF-derived metal phosphides.[120] Collectively, these

Table 2 Summary of Earth-abundant metal complexes and MOF-based catalysts reported for the HER, OER, and bifunctional water splitting, including key catalytic performance data

Catalyst	Electrolyte	HER (η_{10}, mV)	OER (η_{10}, mV)	Cell voltage (V)	Ref.
TImCoPc/KB (3.5 : 1.5)	0.5 M H_2SO_4	−108	—	—	52
NENU-500	0.5 M H_2SO_4	−237	—	—	96
AB&CTGU-5	0.5 M H_2SO_4	−44	—	—	97
MoC@GS(700)	1.0 M KOH	−77	—	—	98
poly[CoOTPc] + KB (3.5 : 1.5)	0.5 M H_2SO_4	−79	—	—	3
UiO-66–NH_2–Mo-5	0.5 M H_2SO_4	−200	—	—	99
Pd(II)TNPc + KB	0.5 M H_2SO_4	−187	—	—	100
Co–N–GA	1.0 M PBS	−299	—	—	101
NiS_2 HMSs	1.0 M KOH	−219	—	—	102
Poly[$Co^{(II)}$THTPc] : KB (4 : 1)	1.0 M KOH	—	359	—	103
$Mn_{0.52}Fe_{0.71}$Ni–MOF-74	1.0 M KOH		267 (at η_{100})	—	104
Ni/FeVAPc	1.0 M KOH	—	312	—	105
CoMM	1.0 M KOH		351		106
CoTTPc/MWCNTs	1.0 M KOH		305		107
Co–MOF	1.0 M KOH		280	—	108
CoOBrPc + KB (4 : 1)	1.0 M KOH	—	381 (GCE) 330 (NF)		62
HQCoPc + KB	HER: 0.5 M H_2SO_4 OER: 1.0 M KOH	−76 (onset)	360	—	109
The rGO : FeSPc/GCE	HER: 0.5 M H_2SO_4 OER: 1.0 M KOH	−93	350	—	110
Co/Co_9S_8@ SNGS-1000	0.1 M KOH	−350 (at η_{20})	290	1.58 (at η_{20})	81
3D-CNTA	1.0 M KOH	−185	360	1.68	111
$Co_{0.85}$Se@NC	1.0 M KOH	−230	320	1.76	95
MSZIF-900	HER: 0.5 M H_2SO_4 OER: 1.0 M KOH	−233	337	—	112
$Ni_3ZnC_{0.7}$-550	1.0 M KOH	−93	320	1.65	113
$(Fe_{0.1}Ni_{0.9})_2P$(O)/NF	1.0 M KOH	−87	240 (at η_{100})	1.50	83
UTBrImPc–MWCNT	HER: 0.5 M H_2SO_4 OER: 1.0 M KOH	−15 (onset)	368	—	11
NiFe–MOF array	0.1 M KOH	−134	240	1.55	82
CoS_2 NTA/CC	1.0 M KOH	−193	276	1.67	114
$CoSe_2$/CF	1.0 M KOH	−95	297	1.63	115
NiFe–Se/C	1.0 M KOH	−160	240	1.68	116
(Ni,Co) Se_2/C–HRD	1.0 M KOH	−87	245	1.58	117

studies demonstrate the revolutionary potential of *in situ* spectroscopy in revealing the electronic evolution and dynamic restructuring of electrocatalysts under operating conditions which is frequently unavailable using static *ex situ* techniques. These methods are still underutilized in molecularly defined metal-complex catalysts for water electrolysis, where structural flux and low intermediate lifetimes present particular difficulties, despite their success in MOF-derived systems. To close this gap, a concerted effort must be made to develop multimodal, operando techniques that combine computational, spectroscopic, and electrochemical tools to reveal active-site dynamics and guide the predictive design of catalysts of the future.

4. Conclusion, challenges and future directions

Recent developments in the design of Earth-abundant metal complexes, particularly those based on Fe, Co, Ni, Mn, and Mo, have greatly advanced the field of EWS using bifunctional electrocatalysis. Many of the most successful systems, as covered in this review, rely on cooperative interactions between two or more metal sites rather than the single-metal center. These interactions provide synergistic benefits in terms of stability, catalytic turnover, and charge redistribution. This strategy is demonstrated by representative bimetallic and trimetallic compositions, including Ni–Fe, Co–Ni–Mo, and Fe–Co–Ni phosphides, which exhibit improved kinetics and advantageous adsorption energetics in both the HER and OER regimes. However, even with these positive advancements, the wider use of some abundant elements, especially Mn and Mo, is still relatively unexplored, especially in comparison with the predominance of Co, Ni, and Fe. The gap is indicative of a larger issue facing the field *i.e.*, inadequate utilization of the entire periodic scheme of Earth-abundant, catalytically relevant metals and a lack of systematic compositional mapping. Furthermore, although metal synergism is frequently reported, the actual design space investigated is still small and frequently restricted to a small number of stoichiometries or structural designs. Consequently, multi-metallic tuning, edge site engineering, and ligand environment modulation have not yet researched their full potential. The lack of a thorough mechanistic understanding of these systems under operational conditions is a more basic bottleneck. The specific characteristics and dynamics of the catalytically active sites are still mostly unknown, despite the fact that many catalysts exhibit bifunctional activity. The reason for this is the persistent dependence on *ex situ* characterization methods, which are

unable to account for the real-time surface reconstructions, oxidation-state modifications, and coordination environment changes that take place throughout operation. On the other hand, the use of operando techniques, including electrochemical mass spectrometry, Raman spectroscopy, UV-Vis spectroscopy, and *in situ* XAS, has recently started to uncover the dynamic pathways and transient intermediates driving electrocatalytic turnover. These tools are still not widely used, though, especially when discussing metal complexes that are molecularly defined.

In addition, despite the great value of DFT in clarifying adsorption energetics, PCET kinetics, and d-band tuning techniques, it has not been widely incorporated into experimental procedures. Data-driven, feedback-optimized design cycles are not possible because theoretical predictions are typically separated from material synthesis and testing. Combining computational and experimental frameworks to close this gap could greatly speed up catalyst discovery and logical optimization. Apart from mechanistic clarity, stability and scalability problems interfere with the practical implementation of these materials. Even though a lot of systems show promise in the short term, they frequently degrade over time, especially at high current densities that are pertinent to industrial water electrolysis. Long-term durability is compromised by irreversible phase changes, ligand dissociation, and metal leaching. However, the synthetic procedures for these complexes often entail complex, multi-step processes that are not suitable for large-scale production, such as template-directed growth, high-temperature pyrolysis, or multi-day solvothermal procedures. Addressing these issues in the future will call for a diversified approach. This includes adopting scalable synthetic routes that are compatible with industrial processes, expanding compositional space to include underutilized metals like Mn and Mo, and using operando characterization extensively to track active-state transitions. Furthermore, design rules that go beyond trial-and-error discovery can be unlocked by combining data-driven catalyst screening with high-throughput DFT modelling. For laboratory-scale advancements to be translated into reliable, inexpensive, and scalable technologies for sustainable hydrogen production, these approaches must converge.

Author contributions

Naseem Kousar: conceptualization, methodology, investigation, validation, writing – original draft, and review and editing; Gouthami Patil: conceptualization and data curation; Ashwini Chikkabasur Kumbara: methodology and validation; Basavesh Nisty: review and editing; Rajesh G H: formal analysis; Lokesh Koodlur Sannegowda: supervision, validation, review and editing, and funding acquisition.

Conflicts of interest

The authors declare no competing financial interest.

Data availability

The data supporting this article is included as part of the main manuscript.

Acknowledgements

The authors would like to acknowledge DST-SERB, Govt. of India grant no. DST-FIST (SR/FST/CSI-003/2016), India-Uzbekistan Collaborative Grant (no. INT/Uzbek/P-21), VGST–KFIST grant no. KSTePS/VGST-KFIST (L1)/2017/267 (GRD no. 555) and VSK University Interdisciplinary grant no 849/2 dated 25/08/2022. NK is indebted to KSTePS, DST, Govt. of Karnataka, for the financial assistance. GP is thankful to DST, Govt. of India, for the Inspire fellowship. ACK, BN and RGH are thankful to the Dept. of OBC, Govt. of Karnataka, for financial support.

References

1 I. Hilali, Accelerating the transition to a hydrogen economy: Achieving carbon neutrality, in *Accelerating the Transition to a Hydrogen Economy*, Elsevier, 2025, pp. 105–127. DOI: 10.1016/B978-0-443-24002-7.00009-4.
2 R. Mondal, *et al.*, A spontaneous hydrogen fuel purifier under truly ambient weather conditions, *Energy Environ. Sci.*, 2023, **16**(9), 3860–3872, DOI: 10.1039/D3EE02095A.
3 N. Kousar and L. K. Sannegowda, Hybrid cobalt phthalocyanine polymer as a potential electrocatalyst for hydrogen evolution reaction, *Int. J. Hydrogen Energy*, 2024, **50**, 37–47, DOI: 10.1016/j.ijhydene.2023.06.296.
4 S. Paraschiv, L. S. Paraschiv and A. Serban, Global hydrogen production capacity for sustainable decarbonization and green transition in transport applications to mitigate climate change: a comprehensive overview, *Manage. Environ. Qual.*, 2025, DOI: 10.1108/MEQ-10-2024-0461.
5 Y. Cao, *et al.*, A hierarchical CuO@ NiCo layered double hydroxide core–shell nanoarray as an efficient electrocatalyst for the oxygen evolution reaction, *Inorg. Chem. Front.*, 2021, **8**(12), 3049–3054, DOI: 10.1039/D1QI00124H.
6 X. Chai, *et al.*, Synergistic enhancement of overall seawater splitting by atomic doping and heterostructure interface engineering in W–MoS2@ FeNi2S4/NF catalyst, *Int. J. Hydrogen Energy*, 2025, **101**, 1044–1053, DOI: 10.1016/j.ijhydene.2024.12.507.
7 S. Aralekallu, *et al.*, Hybrid water electrolysis as the way forward to sustainable hydrogen production, *Sustainable Energy Fuels*, 2025, **9**(11), 2928–2940, DOI: 10.1039/D5SE00236B.
8 M. Younas, *et al.*, An overview of hydrogen production: current status, potential, and challenges, *Fuel*, 2022, **316**, 123317, DOI: 10.1016/j.fuel.2022.123317.
9 W. C. Ng, *et al.*, Elevating the prospects of green hydrogen (H2) production through solar-powered water splitting

devices: A systematic review, *Sustainable Mater. Technol.*, 2024, e00972, DOI: 10.1016/j.susmat.2024.e00972.
10 R. Thimmappa, *et al.*, An atmospheric water electrolyzer for decentralized green hydrogen production, *Cell Rep. Phys. Sci.*, 2021, **2**(11), 100627, DOI: 10.1016/j.xcrp.2021.100627.
11 Giddaerappa, *et al.*, Uranium phthalocyanine-anchored acid-functionalized multiwalled carbon nanotubes for water electrolysis, *ACS Appl. Nano Mater.*, 2023, **6**(10), 8880–8893, DOI: 10.1021/acsanm.3c01328.
12 S. Wang, A. Lu and C.-J. Zhong, Hydrogen production from water electrolysis: role of catalysts, *Nano Convergence*, 2021, **8**(1), 4, DOI: 10.1186/s40580-021-00254-x.
13 D. T. Tran, *et al.*, Current status of developed electrocatalysts for water splitting technologies: from experimental to industrial perspective, *Nano Convergence*, 2025, **12**(1), 9, DOI: 10.1186/s40580-024-00468-9.
14 L. Quan, *et al.*, Bifunctional electrocatalysts for overall and hybrid water splitting, *Chem. Rev.*, 2024, **124**(7), 3694–3812, DOI: 10.1021/acs.chemrev.3c00332.
15 Y. Wang, *et al.*, A review on unitized regenerative fuel cell technologies, part-A: Unitized regenerative proton exchange membrane fuel cells, *Renewable Sustainable Energy Rev.*, 2016, **65**, 961–977, DOI: 10.1016/j.rser.2016.07.046.
16 R. Bose, *et al.*, High performance multicomponent bifunctional catalysts for overall water splitting, *J. Mater. Chem. A*, 2020, **8**(27), 13795–13805, DOI: 10.1039/D0TA02697B.
17 Q. Liang, G. Brocks and A. Bieberle-Hütter, Oxygen evolution reaction (OER) mechanism under alkaline and acidic conditions, *J. Phys.: Energy*, 2021, **3**(2), 026001, DOI: 10.1088/2515-7655/abdc85.
18 M. D. Bhatt and J. Y. Lee, Advancement of platinum (Pt)-free (non-Pt precious metals) and/or metal-free (non-precious-metals) electrocatalysts in energy applications: A review and perspectives, *Energy Fuels*, 2020, **34**(6), 6634–6695, DOI: 10.1021/acs.energyfuels.0c00953.
19 X. Cao, T. Wang and L. Jiao, Transition-metal (Fe, Co, and Ni)-based nanofiber electrocatalysts for water splitting, *Adv. Fiber Mater.*, 2021, 1–19, DOI: 10.1007/s42765-021-00065-z.
20 G. Yilmaz, *et al.*, Atomic- and molecular-level design of functional metal–organic frameworks (MOFs) and derivatives for energy and environmental applications, *Adv. Sci.*, 2019, **6**(21), 1901129, DOI: 10.1002/advs.201901129.
21 M. Parmar, *et al.*, Synergistic effects of the substrate–ligand interaction in metal–organic complexes on the de-electronation kinetics of a vitamin C fuel cell, *Dalton Trans.*, 2024, **53**(32), 13384–13393, DOI: 10.1039/D4DT01370K.
22 K. Bera, *et al.*, Enhancement of the OER kinetics of the less-explored α-MnO_2 via nickel doping approaches in alkaline medium, *Inorg. Chem.*, 2021, **60**(24), 19429–19439, DOI: 10.1021/acs.inorgchem.1c03236.
23 Q. Li, *The role of Fe in conjunction with N-doping on oxygen electrocatalysis*, Diss. Queen Mary University of London, 2025.
24 Y. Pan, *et al.*, Modulation Strategies and Activity Descriptors of Spinel Electrocatalysts for Lithium–Oxygen Batteries, *Batteries Supercaps*, 2024, **7**(4), e202300609, DOI: 10.1002/batt.202300609.
25 W. Song, *et al.*, Advances in Stability of NiFe–Based Anodes toward Oxygen Evolution Reaction for Alkaline Water Electrolysis, *Small*, 2024, **20**(48), 2406075, DOI: 10.1002/smll.202406075.
26 F. Bao, *et al.*, Understanding the hydrogen evolution reaction kinetics of electrodeposited nickel–molybdenum in acidic, near–neutral, and alkaline conditions, *ChemElectroChem*, 2021, **8**(1), 195–208, DOI: 10.1002/celc.202001436.
27 L. B. Neon, *Spectroscopic study of supported MoS_2 catalysts for HER electrocatalysis in acidic media*, Diss. Normandie Université, 2023.
28 A. Nandy, *et al.*, Computational discovery of transition-metal complexes: from high-throughput screening to machine learning, *Chem. Rev.*, 2021, **121**(16), 9927–10000, DOI: 10.1021/acs.chemrev.1c00347.
29 A. Nandy, *Using Data-Driven Models to Understand Transition Metal Catalyst Energy Landscapes and Metal-Organic Framework Stability*, Massachusetts Institute of Technology, 2023.
30 A. R. Kottaichamy, *et al.*, Unprecedented energy storage in metal–organic complexes via constitutional isomerism, *Chem. Sci.*, 2023, **14**(23), 6383–6392, DOI: 10.1039/D3SC01692G.
31 J. Guo, *et al.*, Rational Design of Earth–Abundant Catalysts toward Sustainability, *Adv. Mater.*, 2024, **36**(42), 2407102, DOI: 10.1002/adma.202407102.
32 B. Das, *et al.*, Structural features of molecular electrocatalysts in multi-electron redox processes for renewable energy–recent advances, *Sustainable Energy Fuels*, 2019, **3**(9), 2159–2175, DOI: 10.1039/C9SE00280D.
33 S. Dutt, *et al.*, Switchable molecular electrocatalysis, *Chem. Sci.*, 2024, **15**(33), 13262–13270, DOI: 10.1039/D4SC01284D.
34 T. ul Haq and Y. Haik, *Electrochemical Water Splitting*, Springer Nature Singapore, Singapore, 2024.
35 M. Nazari and M. Ghaemmaghami, Approach to evaluation of electrocatalytic water splitting parameters, reflecting intrinsic activity: toward the right pathway, *ChemSusChem*, 2023, **16**(11), e202202126, DOI: 10.1002/cssc.202202126.
36 K. Dastafkan, *Modulating surface and interface chemistry for advancing electrochemical water splitting*, Diss. UNSW Sydney, 2021.
37 D. Xiao, *et al.*, Bio-inspired molecular catalysts for water oxidation, *Catalysts*, 2021, **11**(9), 1068, DOI: 10.3390/catal11091068.
38 N. Mahmood, *et al.*, Electrocatalysts for hydrogen evolution in alkaline electrolytes: mechanisms, challenges, and prospective solutions, *Adv. Sci.*, 2018, **5**(2), 1700464, DOI: 10.1002/advs.201700464.
39 Y. Qiu, *et al.*, Electrocatalysts development for hydrogen oxidation reaction in alkaline media: From mechanism

understanding to materials design, *Chin. J. Catal.*, 2021, **42**(12), 2094–2104, DOI: 10.1016/S1872-2067(21)64088-3.
40 N. Kousar, *et al.*, Substrate-driven electrocatalysis of natural and earth-abundant pyrite towards oxygen evolution reaction, *Electrochim. Acta*, 2024, **475**, 143575, DOI: 10.1016/j.electacta.2023.143575.
41 Y. H. Budnikova, Recent advances in metal–organic frameworks for electrocatalytic hydrogen evolution and overall water splitting reactions, *Dalton Trans.*, 2020, **49**(36), 12483–12502, DOI: 10.1039/D0DT01741H.
42 P. Phogat, *et al.*, Fundamentals of Electrochemistry, in *Electrochemical Devices: Principles to Applications*, Springer Nature Singapore, Singapore, 2024, pp. 1–27. DOI: 10.1007/978-981-96-0527-9_1.
43 R. E. Warburton, A. V. Soudackov and S. Hammes-Schiffer, Theoretical modeling of electrochemical proton-coupled electron transfer, *Chem. Rev.*, 2022, **122**(12), 10599–10650, DOI: 10.1021/acs.chemrev.1c00929.
44 J. Schneider, *et al.*, Determination of proton-coupled electron transfer reorganization energies with application to water oxidation catalysts, *J. Am. Chem. Soc.*, 2019, **141**(25), 9758–9763, DOI: 10.1021/jacs.9b01296.
45 N. Sun, *et al.*, MOF-based electrocatalysts: an overview from the perspective of structural design, *Chem. Rev.*, 2025, **125**(5), 2703–2792, DOI: 10.1021/acs.chemrev.4c00664.
46 S. Jiao, X. Fu and H. Huang, Descriptors for the evaluation of electrocatalytic reactions: d–band theory and beyond, *Adv. Funct. Mater.*, 2022, **32**(4), 2107651, DOI: 10.1002/adfm.202107651.
47 L. G. M. Pettersson and A. Nilsson, A molecular perspective on the d-band model: Synergy between experiment and theory, *Top. Catal.*, 2014, **57**, 2–13, DOI: 10.1007/s11244-013-0157-4.
48 D. Li, *et al.*, Tailoring the d–Band Center over Isomorphism Pyrite Catalyst for Optimized Intrinsic Affinity to Intermediates in Lithium–Oxygen Batteries, *Adv. Energy Mater.*, 2023, **13**(15), 2204057, DOI: 10.1002/aenm.202204057.
49 P. Serp, Cooperativity in supported metal single atom catalysis, *Nanoscale*, 2021, **13**(12), 5985–6004, DOI: 10.1039/D1NR00465D.
50 A. Zhou, *et al.*, Ferrocene-MOFs: Optimizing OER Kinetics for Water Splitting, *Inorg. Chem.*, 2025, **64**(9), 4680–4688, DOI: 10.1021/acs.inorgchem.5c00334.
51 V.-H. Do and J.-M. Lee, Orbital occupancy and spin polarization: from mechanistic study to rational design of transition metal-based electrocatalysts toward energy applications, *ACS Nano*, 2022, **16**(11), 17847–17890, DOI: 10.1021/acsnano.2c08919.
52 A. Chikkabasur Kumbara, N. Kousar and L. K. Sannegowda, Catalytic Reinforcement in Hybrid Imidazole Functionalized Cobalt Phthalocyanine and Ketjenblack for Boosted Hydrogen Evolution, *Chem. – Asian J.*, 2025, **20**(7), e202401090, DOI: 10.1002/asia.202401090.
53 Z. Zhou, *et al.*, Electrocatalytic hydrogen evolution under neutral pH conditions: current understandings, recent advances, and future prospects, *Energy Environ. Sci.*, 2020, **13**(10), 3185–3206, DOI: 10.1039/D0EE01856B.
54 H. Khani, A. R. Puente Santiago and T. He, An interfacial view of cation effects on electrocatalysis systems, *Angew. Chem., Int. Ed.*, 2023, **62**(43), e202306103, DOI: 10.1002/anie.202306103.
55 M. Chatenet, *et al.*, Water electrolysis: from textbook knowledge to the latest scientific strategies and industrial developments, *Chem. Soc. Rev.*, 2022, **51**(11), 4583–4762, DOI: 10.1039/D0CS01079K.
56 L. Grajciar, *et al.*, Towards operando computational modeling in heterogeneous catalysis, *Chem. Soc. Rev.*, 2018, **47**(22), 8307–8348, DOI: 10.1039/C8CS00398J.
57 S. Yang, *et al.*, The mechanism of water oxidation using transition metal-based heterogeneous electrocatalysts, *Chem. Soc. Rev.*, 2024, **53**(11), 5593–5625, DOI: 10.1039/D3CS01031G.
58 A. Corma, H. I. Garcia and F. X. Llabrés i Xamena, Engineering metal organic frameworks for heterogeneous catalysis, *Chem. Rev.*, 2010, **110**(8), 4606–4655, DOI: 10.1021/cr9003924.
59 L. Miao, *et al.*, Computational chemistry for water-splitting electrocatalysis, *Chem. Soc. Rev.*, 2024, **53**(6), 2771–2807, DOI: 10.1039/D2CS01068B.
60 A. Badreldin, O. Bouhali and A. Abdel-Wahab, Complimentary computational cues for water electrocatalysis: A DFT and ML perspective, *Adv. Funct. Mater.*, 2024, **34**(12), 2312425, DOI: 10.1002/adfm.202312425.
61 A. Rana, *et al.*, Activating Fe(I) porphyrins for the hydrogen evolution reaction using second-sphere proton transfer residues, *Inorg. Chem.*, 2017, **56**(4), 1783–1793, DOI: 10.1021/acs.inorgchem.6b01707.
62 N. Kousar, *et al.*, Interfacial Synergism of Brominated Phthalocyanine and Carbon Nanoparticle-Based Nanocomposite for Efficient Oxygen Electrocatalysis, *ACS Appl. Energy Mater.*, 2024, **7**(17), 7545–7559, DOI: 10.1021/acsaem.4c01987.
63 M. W. Drover, A guide to secondary coordination sphere editing, *Chem. Soc. Rev.*, 2022, **51**(6), 1861–1880, DOI: 10.1039/D2CS00022A.
64 Y. Zhang, S. Nurhanna Riduan and J. Wang, Redox active metal–and covalent organic frameworks for energy storage: Balancing porosity and electrical conductivity, *Chem. – Eur. J.*, 2017, **23**(65), 16419–16431, DOI: 10.1002/chem.201702919.
65 Y.-B. Huang, *et al.*, Multifunctional metal–organic framework catalysts: synergistic catalysis and tandem reactions, *Chem. Soc. Rev.*, 2017, **46**(1), 126–157, DOI: 10.1039/C6CS00250A.
66 J. Wang, *et al.*, Non-precious-metal catalysts for alkaline water electrolysis: operando characterizations, theoretical calculations, and recent advances, *Chem. Soc. Rev.*, 2020, **49**(24), 9154–9196, DOI: 10.1039/D0CS00575D.
67 W. Shen, *et al.*, Progress in in situ characterization of electrocatalysis, *EES Catal.*, 2025, **3**(1), 10–31, DOI: 10.1039/D4EY00168K.
68 P. Acharya, *et al.*, Temporal Ni K-edge X-ray absorption spectroscopy study reveals the kinetics of the Ni redox behavior of the iron-nickel oxide bimetallic OER catalyst,

J. Phys. Chem. C, 2023, **127**(25), 11891–11901, DOI: 10.1021/acs.jpcc.3c03480.

69 A. K. Singh and L. Roy, Evolution in the Design of Water Oxidation Catalysts with Transition-Metals: A Perspective on Biological, Molecular, Supramolecular, and Hybrid Approaches, *ACS Omega*, 2024, **9**(9), 9886–9920, DOI: 10.1021/acsomega.3c07847.

70 R. Teixeira, *et al.*, Fluorescence spectroscopy of porphyrins and phthalocyanines: Some insights into supramolecular self-assembly, microencapsulation, and imaging microscopy, *Molecules*, 2021, **26**(14), 4264, DOI: 10.3390/molecules26144264.

71 Y. AlSalka, *et al.*, Electrochemical and photoelectrochemical water splitting: operando Raman and Fourier transform infrared spectroscopy as useful probing techniques, *Energy Technol.*, 2023, **11**(3), 2200788, DOI: 10.1002/ente.202200788.

72 W. Liao, *et al.*, Application of in situ/operando characterization techniques in heterostructure catalysts toward water electrolysis, *Nano Res.*, 2023, **16**(2), 1984–1991, DOI: 10.1007/s12274-022-5048-1.

73 F. Meharban, *et al.*, Scaling up stability: navigating from lab insights to robust oxygen evolution electrocatalysts for industrial water electrolysis, *Adv. Energy Mater.*, 2024, **14**(41), 2402886, DOI: 10.1002/aenm.202402886.

74 J. Foster, *et al.*, X-ray photoelectron spectroscopy investigation of iridium oxide catalyst layers: Insights into the catalyst-ionomer interface, *Electrochim. Acta*, 2025, **517**, 145705, DOI: 10.1016/j.coelec.2019.03.016.

75 X. Deng, *et al.*, Electrochemical imaging uncovers the heterogeneity of HER activity by sulfur vacancies in molybdenum disulfide monolayer, *Chin. Chem. Lett.*, 2025, **36**(3), 110379, DOI: 10.1016/j.cclet.2024.110379.

76 K. Zhao, *et al.*, Recent development and applications of differential electrochemical mass spectrometry in emerging energy conversion and storage solutions, *Chem. Soc. Rev.*, 2024, **53**(13), 6917–6959, DOI: 10.1039/D3CS00840A.

77 A. Wang, *et al.*, Electrochemical hydrogen and oxygen evolution reactions from a cobalt-porphyrin-based covalent organic polymer, *J. Colloid Interface Sci.*, 2020, **579**, 598–606, DOI: 10.1016/j.jcis.2020.06.109.

78 A. Goswami, *et al.*, In situ grown Mn(II) MOF upon nickel foam acts as a robust self-supporting bifunctional electrode for overall water splitting: a bimetallic synergistic collaboration strategy, *ACS Appl. Mater. Interfaces*, 2022, **14**(26), 29722–29734, DOI: 10.1021/acsami.2c04304.

79 H. Guan, *et al.*, FeMn bimetallic MOF directly applicable as an efficient electrocatalyst for overall water splitting, *Colloids Surf., A*, 2021, **624**, 126596, DOI: 10.1016/j.colsurfa.2021.126596.

80 M. Liu, *et al.*, Overall water–splitting electrocatalysts based on 2D CoNi–metal–organic frameworks and its derivative, *Adv. Mater. Interfaces*, 2018, **5**(21), 1800849, DOI: 10.1002/admi.201800849.

81 X. Zhang, *et al.*, Co/Co9S8@ S, N-doped porous graphene sheets derived from S, N dual organic ligands assembled Co-MOFs as superior electrocatalysts for full water splitting in alkaline media, *Nano Energy*, 2016, **30**, 93–102, DOI: 10.1016/j.nanoen.2016.09.040.

82 J. Duan, S. Chen and C. Zhao, Ultrathin metal-organic framework array for efficient electrocatalytic water splitting, *Nat. Commun.*, 2017, **8**(1), 15341, DOI: 10.1038/ncomms15341.

83 C. Lin, *et al.*, Construction of an iron and oxygen co-doped nickel phosphide based on MOF derivatives for highly efficient and long-enduring water splitting, *J. Mater. Chem. A*, 2020, **8**(8), 4570–4578, DOI: 10.1039/C9TA13583A.

84 G. Yang, *et al.*, Phosphidation treatment of surfactant-tuned iron polyphthalocyanine grown in situ on nickel foam: An efficient bifunctional catalyst for overall water splitting, *Int. J. Hydrogen Energy*, 2024, **55**, 153–163, DOI: 10.1016/j.ijhydene.2023.11.121.

85 Q. Mou, *et al.*, A bimetal hierarchical layer structure MOF grown on Ni foam as a bifunctional catalyst for the OER and HER, *Inorg. Chem. Front.*, 2021, **8**(11), 2889–2899, DOI: 10.1039/D1QI00267H.

86 F. S. Farahani, *et al.*, Trilayer metal–organic frameworks as multifunctional electrocatalysts for energy conversion and storage applications, *J. Am. Chem. Soc.*, 2022, **144**(8), 3411–3428, DOI: 10.1021/jacs.1c10963.

87 Z. Fan, *et al.*, Rational design of ruthenium and cobalt-based composites with rich metal–insulator interfaces for efficient and stable overall water splitting in acidic electrolyte, *ACS Appl. Mater. Interfaces*, 2019, **11**(51), 47894–47903, DOI: 10.1021/acsami.9b15844.

88 D. Das, S. Santra and K. K. Nanda, In situ fabrication of a nickel/molybdenum carbide-anchored N-doped graphene/CNT hybrid: an efficient (pre) catalyst for OER and HER, *ACS Appl. Mater. Interfaces*, 2018, **10**(41), 35025–35038, DOI: 10.1021/acsami.8b09941.

89 Y. Li, *et al.*, MOF-derived Mn doped porous CoP nanosheets as efficient and stable bifunctional electrocatalysts for water splitting, *Dalton Trans.*, 2018, **47**(41), 14679–14685, DOI: 10.1039/C8DT02706D.

90 X. Shi, *et al.*, A "MOFs plus MOFs" strategy toward Co–Mo 2 N tubes for efficient electrocatalytic overall water splitting, *J. Mater. Chem. A*, 2018, **6**(41), 20100–20109, DOI: 10.1039/C8TA07906D.

91 J. Sun, *et al.*, Iron–cobalt–nickel trimetal phosphides as high-performance electrocatalysts for overall water splitting, *Sustainable Energy Fuels*, 2020, **4**(9), 4531–4537, DOI: 10.1039/D0SE00694G.

92 Q. Liang, *et al.*, Metal-organic frameworks derived reverse-encapsulation Co-NC@ Mo2C complex for efficient overall water splitting, *Nano Energy*, 2019, **57**, 746–752, DOI: 10.1016/j.nanoen.2018.12.060.

93 Y. Pan, *et al.*, Core–shell ZIF-8@ ZIF-67-derived CoP nanoparticle-embedded N-doped carbon nanotube hollow polyhedron for efficient overall water splitting, *J. Am. Chem. Soc.*, 2018, **140**(7), 2610–2618, DOI: 10.1021/jacs.7b12420.

94 W. Chen, *et al.*, Plasma-engineered bifunctional cobalt–metal organic framework derivatives for high-performance complete water electrolysis, *Nanoscale*, 2021, **13**(12), 6201–6211, DOI: 10.1039/D1NR00317H.

95 T. Meng, *et al.*, In situ coupling of Co 0.85 Se and N-doped carbon via one-step selenization of metal–organic frameworks as a trifunctional catalyst for overall water splitting and Zn–air batteries, *J. Mater. Chem. A*, 2017, **5**(15), 7001–7014, DOI: **10.1039/C7TA01453H**.

96 J.-S. Qin, *et al.*, Ultrastable polymolybdate-based metal–organic frameworks as highly active electrocatalysts for hydrogen generation from water, *J. Am. Chem. Soc.*, 2015, **137**(22), 7169–7177, DOI: **10.1021/jacs.5b02688**.

97 Y.-P. Wu, *et al.*, Surfactant–assisted phase–selective synthesis of new cobalt MOFs and their efficient electrocatalytic hydrogen evolution reaction, *Angew. Chem.*, 2017, **129**(42), 13181–13185, DOI: **10.1002/ange.201707238**.

98 Z. Shi, *et al.*, Porous nanoMoC@ graphite shell derived from a MOFs-directed strategy: an efficient electrocatalyst for the hydrogen evolution reaction, *J. Mater. Chem. A*, 2016, **4**(16), 6006–6013, DOI: **10.1039/C6TA01900E**.

99 X. Dai, *et al.*, Molybdenum polysulfide anchored on porous Zr-metal organic framework to enhance the performance of hydrogen evolution reaction, *J. Phys. Chem. C*, 2016, **120**(23), 12539–12548, DOI: **10.1021/acs.jpcc.6b02818**.

100 S. Hadimane, S. Aralekallu and L. K. Sannegowda, Tuning a palladium(II) phthalocyanine embedded hybrid electrocatalyst for the hydrogen evolution reaction, *Sustainable Energy Fuels*, 2024, **8**(8), 1775–1787, DOI: **10.1039/D4SE00202D**.

101 Z. Zhu, *et al.*, Construction of a cobalt-embedded nitrogen-doped carbon material with the desired porosity derived from the confined growth of MOFs within graphene aerogels as a superior catalyst towards HER and ORR, *J. Mater. Chem. A*, 2016, **4**(40), 15536–15545, DOI: **10.1039/C6TA05196K**.

102 T. Tian, *et al.*, Surface anion-rich NiS 2 hollow microspheres derived from metal–organic frameworks as a robust electrocatalyst for the hydrogen evolution reaction, *J. Mater. Chem. A*, 2017, **5**(39), 20985–20992, DOI: **10.1039/C7TA06671F**.

103 N. Kousar, *et al.*, Phthalocyanine polymer anchored Ketjen black nanoparticles for bifunctional oxygen electrocatalysis, *ACS Appl. Nano Mater.*, 2024, **7**(9), 10600–10613, DOI: **10.1021/acsanm.4c01044**.

104 W. Zhou, *et al.*, Trimetallic MOF–74 films grown on Ni foam as bifunctional electrocatalysts for overall water splitting, *ChemSusChem*, 2020, **13**(21), 5647–5653, DOI: **10.1002/cssc.202001230**.

105 G. Patil, S. Daniel and L. K. Sannegowda, Elevating Oxygen Evolution using Iron Phthalocyanine Infused Vanillic acid Electrocatalyst, *Chem. – Eur. J.*, 2024, **30**(51), e202401759, DOI: **10.1002/chem.202401759**.

106 P. Kumar, *et al.*, High-density cobalt single-atom catalysts for enhanced oxygen evolution reaction, *J. Am. Chem. Soc.*, 2023, **145**(14), 8052–8063, DOI: **10.1021/jacs.3c00537**.

107 A. C. Kumbara, N. Kousar and L. K. Sannegowda, Bioinspired cobalt phthalocyanine hybrid as bifunctional electrocatalyst for oxygen electrocatalysis, *J. Energy Storage*, 2024, **97**, 112920, DOI: **10.1016/j.est.2024.112920**.

108 R. K. Tripathy, A. K. Samantara and J. N. Behera, A cobalt metal–organic framework (Co-MOF): a bi-functional electro active material for the oxygen evolution and reduction reaction, *Dalton Trans.*, 2019, **48**(28), 10557–10564, DOI: **10.1039/C9DT01730E**.

109 Giddaerappa, *et al.*, Cobalt Phthalocyanine Based Metal–Organic Framework as an Efficient Bifunctional Electrocatalyst for Water Electrolysis, *Energy Fuels*, 2024, **38**(9), 8249–8261, DOI: **10.1021/acs.energyfuels.4c00037**.

110 S. Daniel, *et al.*, Unleashing the Bifunctional Activity of Iron Phthalocyanine–Reduced Graphene Oxide Hybrid for Water Electrolysis, *Energy Fuels*, 2025, **39**(6), 3319–3330, DOI: **10.1021/acs.energyfuels.4c05344**.

111 S. Wang, *et al.*, Metal–organic framework-induced construction of actiniae-like carbon nanotube assembly as advanced multifunctional electrocatalysts for overall water splitting and Zn-air batteries, *Nano Energy*, 2017, **39**, 626–638, DOI: **10.1016/j.nanoen.2017.07.043**.

112 G. Jia, *et al.*, Three–dimensional hierarchical architectures derived from surface–mounted metal–organic framework membranes for enhanced electrocatalysis, *Angew. Chem.*, 2017, **129**(44), 13969–13973, DOI: **10.1002/ange.201708385**.

113 Y. Wang, *et al.*, Cation modulating electrocatalyst derived from bimetallic metal–organic frameworks for overall water splitting, *J. Mater. Chem. A*, 2017, **5**(13), 6170–6177, DOI: **10.1039/C7TA00692F**.

114 C. Guan, *et al.*, Metal–organic framework derived hollow CoS2 nanotube arrays: an efficient bifunctional electrocatalyst for overall water splitting, *Nanoscale Horiz.*, 2017, **2**(6), 342–348, DOI: **10.1039/C7NH00079K**.

115 C. Sun, *et al.*, Metal–organic framework derived CoSe2 nanoparticles anchored on carbon fibers as bifunctional electrocatalysts for efficient overall water splitting, *Nano Res.*, 2016, **9**, 2234–2243, DOI: **10.1007/s12274-016-1110-1**.

116 B. Xu, *et al.*, Direct selenylation of mixed Ni/Fe metal-organic frameworks to NiFe-Se/C nanorods for overall water splitting, *J. Power Sources*, 2017, **366**, 193–199, DOI: **10.1016/j.jpowsour.2017.09.018**.

117 F. Ming, *et al.*, Hierarchical (Ni, Co) Se2/carbon hollow rhombic dodecahedra derived from metal-organic frameworks for efficient water-splitting electrocatalysis, *Electrochim. Acta*, 2017, **250**, 167–173, DOI: **10.1016/j.electacta.2017.08.047**.

118 J. Jia, *et al.*, Role of cobalt phthalocyanine on the formation of high-valent cobalt species revealed by in situ Raman spectroscopy, *J. Mater. Chem. A*, 2023, **11**(15), 8141–8149, DOI: **10.1039/D2TA10063K**.

119 J. Linke, *et al.*, From Operando Investigations to Implementation of Ni–MOF–74 Oxygen Evolution Electrocatalysts, *Adv. Energy Mater.*, 2025, 2501401, DOI: **10.1002/aenm.202501401**.

120 M. Shi, *et al.*, In situ evolution of MOF-derived C@ NiCoP/NF promotes urea-assisted electrocatalytic hydrogen production, *Appl. Catal., B*, 2025, **371**, 125210, DOI: **10.1016/j.apcatb.2025.125210**.

